



Detrimental vs. beneficial influence of ions during solar (SODIS) and photo-Fenton disinfection of *E. coli* in water: (Bi)carbonate, chloride, nitrate and nitrite effects

Elena Rommozzi^{a,b}, Stefanos Giannakis^{c,*}, Rita Giovannetti^{a,*}, Davide Vione^d, César Pulgarin^b

^a School of Science and Technology, Chemistry Division, University of Camerino, 62032, Camerino MC, Italy

^b School of Basic Sciences (SB), Institute of Chemical Science and Engineering (ISIC), Group of Advanced Oxidation Processes (GPAO), École Polytechnique Fédérale de Lausanne (EPFL), Station 6, CH-1015, Lausanne, Switzerland

^c Universidad Politécnica de Madrid (UPM), E.T.S. Ingenieros de Caminos, Canales y Puertos, Departamento de Ingeniería Civil: Hidráulica, Energía y Medio Ambiente, Unidad docente Ingeniería Sanitaria, c/ Profesor Aranguren, s/n, ES-28040, Madrid, Spain

^d Dipartimento di Chimica, Università di Torino, Via P. Giuria 5, 10125, Torino, Italy

ARTICLE INFO

Keywords:

Solar disinfection
Photo-Fenton process
Bacteria
Inorganic ions
Inactivation modeling

ABSTRACT

In this work, we studied the effect of inorganic ions occurring in natural waters on *E. coli* inactivation by solar and photo-Fenton processes, two crucial methods for drinking water treatment in sunny or developing countries. HCO_3^- , Cl^- , SO_4^{2-} , NO_3^- , NO_2^- and NH_4^+ were assessed at relevant concentrations for their inhibiting or facilitating role. The inactivation enhancement during solar disinfection (SODIS) was mainly attributed to the generation of HO^\bullet radicals produced during by excitation of NO_3^- , NO_2^- , while the HO^\bullet of photo-Fenton may be transformed into other radical species in presence of ions. Natural organic matter (NOM) was found to enhance both processes but also to hinder most of the enhancing ions, except for NO_2^- ; modeling with the APEX software unveiled the inter-relations in the presence of NOM, and the possible inactivation activity by NO_2^- . The photo-Fenton inactivation was more significantly enhanced by ions than SODIS (besides the case of NO_3^- , NO_2^-), but both processes were found robust enough.

1. Introduction

Waterborne pathogens causing diseases constitute one of the acute health risks associated with urban wastewater discharge and reuse. They have been identified as a major infection risk in streams, rivers and estuaries. The use of solar radiation to disinfect water, more known as the solar disinfection process (SODIS), has been successfully evaluated as a way to eliminate pathogens from waters destined for consumption [1,2]. Unfortunately, SODIS is prone to temperature dependence and has shown possible bacterial regrowth issues [3–5]. The attempts to enhance the SODIS efficiency focused on low-cost technological or physicochemical modifications [4,6–9], aimed at decreasing the exposure time needed to achieve “permanent” microorganism elimination. This is the rationale for trying to achieve acceleration of the SODIS kinetic performance with the addition of H_2O_2 to raw water, or with the photo-Fenton process [6,10–13]. H_2O_2 directly attacks the

cellular membrane, increasing its permeability and affecting cell survival. It can also diffuse into the cell and initiate an intra-cellular process of cell death [14,15]. The photo-Fenton process involves the reaction of H_2O_2 with photogenerated Fe^{2+} ions, leading to the formation of Reactive Oxygen Species (ROS), such as HO^\bullet radicals. The latter are powerful oxidizing species that can achieve inactivation of bacteria and viruses [12,16,17]. Moreover, the photo-Fenton reagents can also trigger intracellular events due to the transport of iron and H_2O_2 inside cells [18].

Natural water sources have an important content of Natural Organic Matter (NOM) and inorganic ions, such as HCO_3^- , NO_3^- , NO_2^- , Cl^- , SO_4^{2-} and NH_4^+ . These can be naturally present, or be introduced in natural cycles by agricultural, domestic and industrial activities, and have been shown to play a role in photochemical and disinfection processes [19–21] (the mean chemical composition of different water sources can be found in Table 1). In general, NOM and some inorganic ions

Abbreviations: APEX, Aqueous Photochemistry of Environmentally occurring Xenobiotics; CFU, Colony Forming Unit; LB, Luria-Bertani; LMCT, Ligand-to-Metal Charge Transfer; MQ, Milli-Q water; NOM, Natural Organic Matter; PCA, Plate Count Agar; RHS, Reactive Halogen Species; ROS, Reactive Oxygen Species; SRNOM, Suwanee River Natural Organic Matter; UV, Ultraviolet

* Corresponding authors.

E-mail addresses: stefanos.giannakis@upm.es (S. Giannakis), rita.giovannetti@unicam.it (R. Giovannetti).

<https://doi.org/10.1016/j.apcatb.2020.118877>

Received 9 December 2019; Received in revised form 6 February 2020; Accepted 10 March 2020

Available online 12 March 2020

0926-3373/© 2020 The Authors. Published by Elsevier B.V. This is an open access article under the CC BY license

(<http://creativecommons.org/licenses/by/4.0/>).

Table 1

Mean ionic composition of water sources frequently used for Solar disinfection (SODIS) [53–57]. ND = not determined.

Ions	River Water (mg L ⁻¹)	Lake Water (mg L ⁻¹)	Harvested rainwater (mg L ⁻¹)	Groundwater (mg L ⁻¹)
HCO ₃ ⁻	20 – 100	10 – 110	ND	20 – 800
NO ₃ ⁻	0.05 – 4	0.1 – 4	1.56 – 7.04	0.05 – 60
NO ₂ ⁻	< 0.4	< 0.4	0.01 – 0.27	< 1
Cl ⁻	4 – 12	2 – 15	1.48 – 79	2 – 700
SO ₄ ²⁻	0 – 230	2 – 250	1.6 – 15.62	0 – 630
NH ₄ ⁺	< 0.2	0.003 – 0.8	0.06 – 1.4	0.001 – 3

naturally present in water sources can be involved in the absorption of incident sunlight [19,22,23], hence interfering with photo-initiated bacterial inactivation. On the other hand, the Fenton process proceeds mainly via the generation of HO[•], which can be scavenged by both NOM and some ionic species [20,24]. Furthermore, PO₄³⁻ induces the formation of insoluble FePO₄ [24–26] and, by so doing, it can out-weight the effect of all the other ionic species on the photo-Fenton process [24,27,28]. The scavenging of HO[•] by Cl⁻ and Br⁻ follows the same general mechanism (Eqs. 1–5) [29,30], but the process in the presence of chloride proceeds up to Eq. (5) only at acidic pH. At neutral to basic conditions, it does not go beyond Eq. (1) and HClO^{•-} yields back HO[•] + Cl⁻ [31]. Moreover, SO₄²⁻ and F⁻ retard the Fenton process by affecting the Fe³⁺ -ion coordination [32].



In the above reactions, X is a halogen and the relevant species are halide ions and Reactive Halogen Species (RHS). The generation of RHS could still lead to microorganism disinfection [33], as they retain oxidizing power [29,34]. Although less reactive and more selective than HO[•], their reaction mechanism involves pathways such as one-electron oxidation or addition to unsaturated C–C bonds [29,35]. The HO[•] radicals are scavenged with second-order reaction rate constants in the order of 10⁴ M⁻¹ s⁻¹ for H₂PO₄⁻ and 10⁶ M⁻¹ s⁻¹ for HCO₃⁻. However, the rate constants can be as high as 10⁸ M⁻¹ s⁻¹ for CO₃²⁻ and Fe²⁺ [36], 10⁹ M⁻¹ s⁻¹ for Cl⁻ [37] (but the actual outcome for chloride is pH-dependent as mentioned above), and even 10¹⁰ M⁻¹ s⁻¹ for NO₂⁻ and Br⁻ [38].

Dissolved ions have also the potential to enhance either SODIS or photo-Fenton. Examples include the generation of HO[•] by the illumination of NO₃⁻/NO₂⁻ [39,40], or the complexation reactions of Fe²⁺ or Fe³⁺ with inorganic ligands. The latter can affect the distribution and reactivity of the iron species [22,32,41,42]. Hence, depending on their concentration, speciation or distribution, inorganic ions can have contrasting effects on both SODIS and the photo-Fenton processes.

Moreover, the organic matter in solution (NOM) has a double activity as an antagonist or a facilitator of the photo-chemical processes [43–45]. Its presence under sunlight enables a large variety of photo-chemical reactions that proceed by energy transfer and result in singlet oxygen and radical species generation. Such reactions also yield additional ROS such as superoxide and H₂O₂ [45–47]. NOM has the potential to increase the efficiency of both SODIS and photo-Fenton processes, by providing effective ligands that trigger Ligand-to-Metal Charge Transfer (LMCT) processes and produce ligand radicals, ROS and further Fe²⁺ [41,45,48–50]. However, as almost every organic compound, NOM has oxidizable moieties that have the potential to significantly scavenge the photo-produced reactive species [51,52]. NOM is also able to absorb sunlight, but the path lengths of radiation in water during SODIS are never too high and the absorption effect is less

important compared to other contexts, such as the water column of natural aquatic environments.

The above phenomena can explain the intrinsic inconsistencies of the literature about the roles of ions and organic matter in water disinfection, as well as the lack of a systematic investigation. For these reasons, the main goal of this work is to unveil the effect of a series of inorganic ions, namely HCO₃⁻, NO₃⁻, NO₂⁻, Cl⁻, SO₄²⁻ and NH₄⁺, in the absence and in the presence of NOM, on *E. coli* inactivation by the SODIS and photo-Fenton processes. To attain this goal, for each ion under scrutiny, the related chemical events that could result in bacterial inactivation were reviewed, thereby contextualizing our disinfection experiments with the current understanding of natural-water photo-chemistry. The bacterial cultivability as well as the effect of ions concentration during solar exposure and photo-Fenton processes was evaluated, i.e., in presence or absence of the ions. A systematic kinetic assessment will describe the critical parameters in defining bacterial inactivation, namely lag phase and inactivation rate, while the potential role of secondary radicals will be elucidated. In some cases, the changes in lag phase and inactivation kinetics could be modeled, to estimate the effectiveness of photoinduced disinfection as a function of the ions' concentration in sunlit natural waters.

2. Materials and methods

2.1. Chemicals and reagents

The effect of Na⁺ as counter ion is negligible because it is harmless for *E. coli* and cannot absorb sunlight. Therefore, sodium-based salts were used as sources of the ions under scrutiny. The used salts were NaHCO₃, NaNO₃, NaNO₂, NaCl, Na₂SO₄ and (NH₄)₂SO₄ (the latter as source of ammonium, *vide infra* for the rationale of the choice), all supplied by Sigma-Aldrich. Aqueous solutions of salts, in appropriate concentrations, were prepared in Milli-Q water (MQ). FeSO₄·7H₂O and H₂O₂ 30 % w/v (Sigma-Aldrich) was used to prepare the stock solutions of the photo-Fenton reagents (1000 ppm each).

2.2. Photochemical experiments

Solar irradiation with intensity of 620 W m⁻² was simulated by an Atlas SUNTEST Solar simulator. Irradiation experiments at 350 rpm of agitation by magnetic bars placed on stirrer plates and at room temperature were performed, testing the effects on bacteria of HCO₃⁻ at concentrations from 5 to 100 mg L⁻¹, NO₃⁻ from 1 to 50 mg L⁻¹, NO₂⁻ from 0.01 to 5 mg L⁻¹, Cl⁻ from 1 to 500 mg L⁻¹, SO₄²⁻ from 10 to 500 mg L⁻¹ and NH₄⁺ from 0.1 to 10 mg L⁻¹. The salts and their concentrations have been selected in accordance to the actual ions' presence in natural waters, according to Table 1.

In order to define the bacterial survival in the presence of the maximum concentrations of these ions, control experiments after 240 min in dark conditions were performed. In photo-Fenton experiments, the concentration of Fe²⁺ and H₂O₂ solutions were 1 mg L⁻¹ and 10 mg L⁻¹ respectively.

A depiction of the experimental set-up is given in the supplementary material (Scheme S1). The test took place in Pyrex glass reactors with Milli-Q water at near neutral starting pH. The reactors contained 100 mL of *E. coli* dispersion with concentration of 10⁶ colony forming units per mL (CFU mL⁻¹). Before every experiment, reactors were sterilized by autoclaving and after each experiment, reactors were washed with acid to ensure iron removal, with ethanol to remove any other contaminant and finally with deionized water in abundant amounts.

2.3. Bacterial strain and growth media

The bacterial strain used in this study was *E. coli* K12, a non-pathogenic wild-type strain, which can be handled with little genetic

manipulation; *E. coli* strain storage is ensured in cryo-vials containing 20 % of glycerol at -20°C . Bacterial pre-cultures were obtained by spreading 20 μL of the strain into Plate Count Agar (PCA; Merck) followed by 24 h of incubation at 37°C (Heraeus Instruments). A grown colony was then sampled and spread again on a new PCA plate for concentration purposes. After an additional 24 h of incubation at 37°C , the master plate was ready and stored at 4°C ; due to the uncertainty of the dispersion method, the process was done in duplicate.

In order to prepare the bacterial stock solution, a colony of bacteria was extracted from the master plate and inoculated into 5 mL of Luria-Bertani (LB) Broth. Specifically, LB consisted of 10 g L^{-1} tryptone, 10 g L^{-1} NaCl and 5 g L^{-1} yeast extract in Milli-Q water. The saline solution was a sterile NaCl/KCl solution (8 g L^{-1} NaCl and 0.8 g L^{-1} KCl at pH 7–7.5). After a strong mixing by a vortex machine for 1 or 2 min, it was incubated inside a 37°C temperature-controlled room for 8 h and constantly agitated by circular movement at 750 rpm. After 8 h, 2.5 mL of sample were diluted in 250 mL of LB Broth and incubated for 15 h in the same room to ensure that the stationary physiological phase was reached. A 25 mL aliquot of this bacterial sample was separated during the stationary growth phase by centrifugation and was washed 3 times with saline solution. Washing took place in a 4°C centrifuge (Hermle Z 323 K, Renggli Laboratory Systems), at 5000 rpm for 15 min the first time and 5 min the remaining two, with 10 mL of saline solution. After the final wash, 25 mL of clean saline solution was added to the bacterial pellet. This procedure resulted in a bacterial dispersion of approximately 10^9 CFU mL^{-1} .

2.4. Sampling and bacterial enumeration

Samples of 1 mL were taken from the body of the reactor under stirring and placed in sterile plastic Eppendorf vials, to ensure their sterile preservation. In order to obtain information about the disinfection kinetics, sampling was performed at time intervals of 0, 30, 60, 90, 120, 180 and 240 min for SODIS, and at time intervals of 0, 20, 40, 60, 90 and 120 min for photo-Fenton. For reproducibility, each experiment was carried out at least in duplicate (biological/chemical replicates) in double series (statistical replicates) and using 2 or 3 serial dilutions (technical replicates), to achieve measurable bacterial count on the plates; the optimal colony counts in this method are among 15–150. Total inactivation was considered achieved when no bacteria colony was observed any longer in the plates after treatment. The spread plate technique was performed on PCA, contained in plastic sterile Petri dishes, by injecting drop-by-drop 100 μL of samples. The detection limit was 1 CFU mL^{-1} for undiluted samples and 10 CFU mL^{-1} for diluted ones [58]. The incubation period was 18–24 hours at 37°C .

2.5. Data treatment and APEX modeling

In order to model the bacterial response under the solar light and photo-Fenton stress, a 60-min and a 30-min lag period was considered for SODIS and photo-Fenton processes, respectively. After this period, log-linear kinetics were fitted by the GInaFiT freeware add-on for Microsoft Excel [59]. For the kinetic modeling, a log-linear equation with delay was used; its calculation was possible for all cases and it provided the exact time of delay and the subsequent log-linear kinetics of inactivation. The “Shoulder log-linear model” was formulated as shown in Eq. (1) [59].

$$\log_{10}(N) = \log_{10}(N_0) - k^* \frac{t - t_s}{\ln(10)} - \log_{10}[1 + (\exp(k^* t_s) - 1) \exp(-k^* t)] \quad (6)$$

where:

N is the bacterial population at any given time (CFU mL^{-1}).

N_0 is the initial bacterial population (CFU mL^{-1}).

t is the investigated time (s).

t_s is the length of the shoulder period or threshold time to observe inactivation (s).

k is the rate constant of the inactivation (s^{-1}).

In some cases, it was possible to apply photochemical modeling to get better insight into the functioning of some SODIS systems leading to bacterial inactivation. Eq. (6) or its non-logarithmic equivalent was the basis for modeling. At the moment, photochemical modeling can only take into account exogenous inactivation of *E. coli* by reactive transient species (HO^{\bullet} , $^1\text{O}_2$, $^3\text{NOM}^*$), thereby excluding the endogenous process driven by light only [47,60]. In particular, the value of (exogenous) t_s was determined according to the following phenomenological equation, where t_s is expressed in min and $[\text{HO}^{\bullet}]$ in mol L^{-1} [47]:

$$t_s = 158e^{-(3 \times 10^{13} [\text{HO}^{\bullet}])} \quad (7)$$

The value of the steady-state $[\text{HO}^{\bullet}]$ was assessed by means of the APEX software (Aquatic Photochemistry of Environmentally-occurring Xenobiotics) [61] which was also used to determine k as the rate constant of exogenous inactivation by HO^{\bullet} , $^1\text{O}_2$, and $^3\text{NOM}^*$ together. To predict the exogenous threshold time via $[\text{HO}^{\bullet}]$ and the exogenous photo-inactivation rate constants after the lag phase, APEX needs photo-reactivity parameters (the second-order inactivation rate constants of *E. coli* by HO^{\bullet} , $^1\text{O}_2$, and $^3\text{NOM}^*$ [60]), sunlight irradiance, and data of water chemistry and depth [61]. APEX calculates the absorption of radiation by the photosensitizers (NOM, nitrate and nitrite) on the basis of competition for sunlight irradiance, in a Lambert-Beer approach [62]. In the model, NOM is a photochemical source of HO^{\bullet} , $^1\text{O}_2$, and $^3\text{NOM}^*$ as well as a HO^{\bullet} sink, while nitrate and nitrite are both HO^{\bullet} sources. The model results apply to well-mixed waters and provide average values over the whole water column, with contributions from the well-illuminated surface layer and from darker water in the lower depths [63].

It should be underlined that APEX modeling of bacterial inactivation still has several gaps, which presently limit the comparison with experimental results. The main limitations are the following: (i) it is presently not possible to model photo-Fenton, thus APEX is currently limited to pure SODIS; (ii) the model takes into account exogenous inactivation only, thereby neglecting the very important endogenous process. By so doing, model results are bound to underestimate actual photoinactivation; (iii) the model uses summertime sunlight as the radiation source in place of the experimental lamp, which is very useful to simulate field SODIS but further limits comparison with laboratory results; (iv) it is presently not possible to assess the scavenging of HO^{\bullet} by the bacteria. This issue prevents a proper treatment of the systems that contain only bacteria + NO_3^- or bacteria + NO_2^- , in the absence of additional HO^{\bullet} scavengers such as NOM. Despite these limitations, in some cases the model can provide a semi-quantitative insight into the photoinduced processes, which may give interesting indications as far as the inactivation pathways are concerned.

2.6. Chemical and analytical methods

According to the standard methods for water analysis [64], NO_3^- determination (Standard Method 4500 - NO_3^- B) was carried out using a Shimadzu UV-1800 spectrophotometer with a minimum detectable NO_3^- concentration of 0.5 mg L^{-1} while HCO_3^- , expressed as alkalinity (Standard Method 2320 B), was measured by potentiometric titration with H_2SO_4 . NH_4^+ and SO_4^{2-} were analyzed with a HACH DR 3900 spectrophotometer: NH_4^+ was measured using LCK 305 Ammonium-Nitrogen cuvettes (minimum detectable NH_4^+ concentration of 1 mg L^{-1}) while SO_4^{2-} was measured using HACH LCK 153 Sulfate cuvettes (minimum detectable SO_4^{2-} concentration of 40 mg L^{-1}). NO_2^- and Cl^- were analyzed by Quantofix semi quantitative strips (Macherey-Nagel, Germany); NO_2^- was determined with Quantofix nitrite 3000 (minimum detectable NO_2^- concentration of 0.1 mg L^{-1}) while Cl^- was determined with Quantofix chloride 91321 detectable Cl^- concentrations of 0–3000 mg L^{-1} . The pH evolution during treatments was

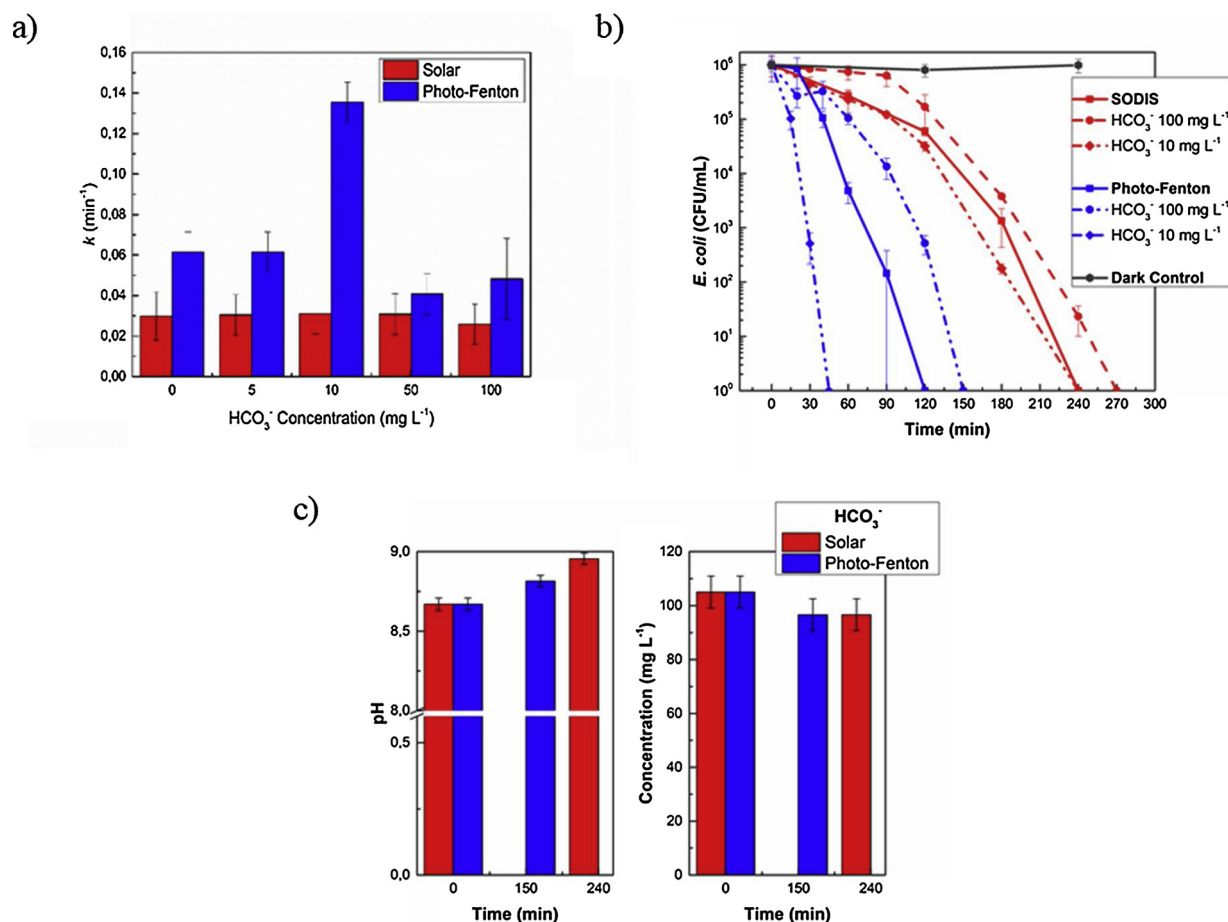


Fig. 1. Kinetic constant values at different HCO_3^- concentrations, in both SODIS and photo-Fenton processes (a). Disinfection experiments with HCO_3^- (b). Changes of pH and HCO_3^- concentration in both processes (c). The detailed disinfection results for SODIS and photo-Fenton in presence of HCO_3^- are presented in Fig. S1.

recorded using a pH-meter manufactured by Mettler Toledo.

3. Results and discussion

3.1. Ions influence on SODIS and photo-Fenton processes

3.1.1. HCO_3^- effects

Fig. 1 summarizes the bicarbonate-related disinfection tests and the effect of the bicarbonate ion in both SODIS and the photo-Fenton process. Fig. 1(a) shows the pseudo-first order kinetic constant values calculated for both processes, at all the tested HCO_3^- concentrations, while Fig. 1(b) shows the most significant disinfection graphs.

The results show that the effect of HCO_3^- on SODIS and the photo-Fenton process is not totally straightforward. First, there is very limited effect on the first-order disinfection rate constants, except for HCO_3^- at 10 mg L⁻¹ in the case of photo-Fenton. There is some more effect on the lag times, although the variation is not linear with HCO_3^- concentration. In terms of overall disinfection, the inactivation of bacteria was faster with 10 mg L⁻¹ HCO_3^- compared to no bicarbonate, and slower with 100 mg L⁻¹ HCO_3^- (Fig. 1(b)).

Fig. 1(c) shows pH and HCO_3^- concentration changes during both SODIS and photo-Fenton. With 100 mg L⁻¹ HCO_3^- , the initially basic pH increased in both cases with a simultaneous decrease of HCO_3^- concentration (~10 mg L⁻¹). In contrast, at 10 mg L⁻¹ HCO_3^- , the pH was near neutral and showed no shift during the reaction (data not shown).

Carbonate and bicarbonate ions are the main inorganic carbon forms in water; most of the HCO_3^- and CO_3^{2-} ions originate from the dissolution of carbonate minerals, the decomposition of organic matter, the respiration of aquatic animals and the exchanges in the carbon cycle

[65]. Due to its high solubility, HCO_3^- is widely distributed in natural waters (see Table 1) and in biological systems, where it constitutes the main biological buffer.

Both HCO_3^- and CO_3^{2-} react with the hydroxyl radicals, HO^\bullet , to yield the carbonate radical $\text{CO}_3^{\bullet-}$ [66]. The latter has oxidizing power as well, although it is more selective compared to HO^\bullet . This phenomenon may explain the fact that the addition of bicarbonate affected the HO^\bullet -producing photo-Fenton process, to a larger extent compared to SODIS (see Fig. 1b). When reacting as an oxidant, $\text{CO}_3^{\bullet-}$ yields back HCO_3^- / CO_3^{2-} . Therefore, the observed changes in HCO_3^- concentration (if any) are closely linked to the interconversion process $\text{HCO}_3^- \rightleftharpoons \text{CO}_3^{2-} + \text{H}^+$ that depends on pH.



The disinfection lag time of *E. coli* has been shown to mainly depend on irradiation and the attack by HO^\bullet [60,67]. Moreover, bacteria could be susceptible to the combined effects of irradiation, basic pH and the presence of oxidizing species. Therefore, pH changes in case of the addition of bicarbonate at high concentration, combined with the consumption of photogenerated HO^\bullet , could have contrasting effects on the disinfection process and produce non-linear phenomena. In addition, at elevated pH one has enhanced Fe^{3+} precipitation that has the potential to hamper the photo-Fenton process.

While $\text{CO}_3^{\bullet-}$ is a less selective oxidant than HO^\bullet , it has much longer lifetime in aqueous solution and can, therefore, diffuse over a much larger range. The germicidal action of HO^\bullet is limited by its inability to react with cell components other than the membrane, while the longer $\text{CO}_3^{\bullet-}$ lifetime could enable additional disinfection pathways. Indeed,

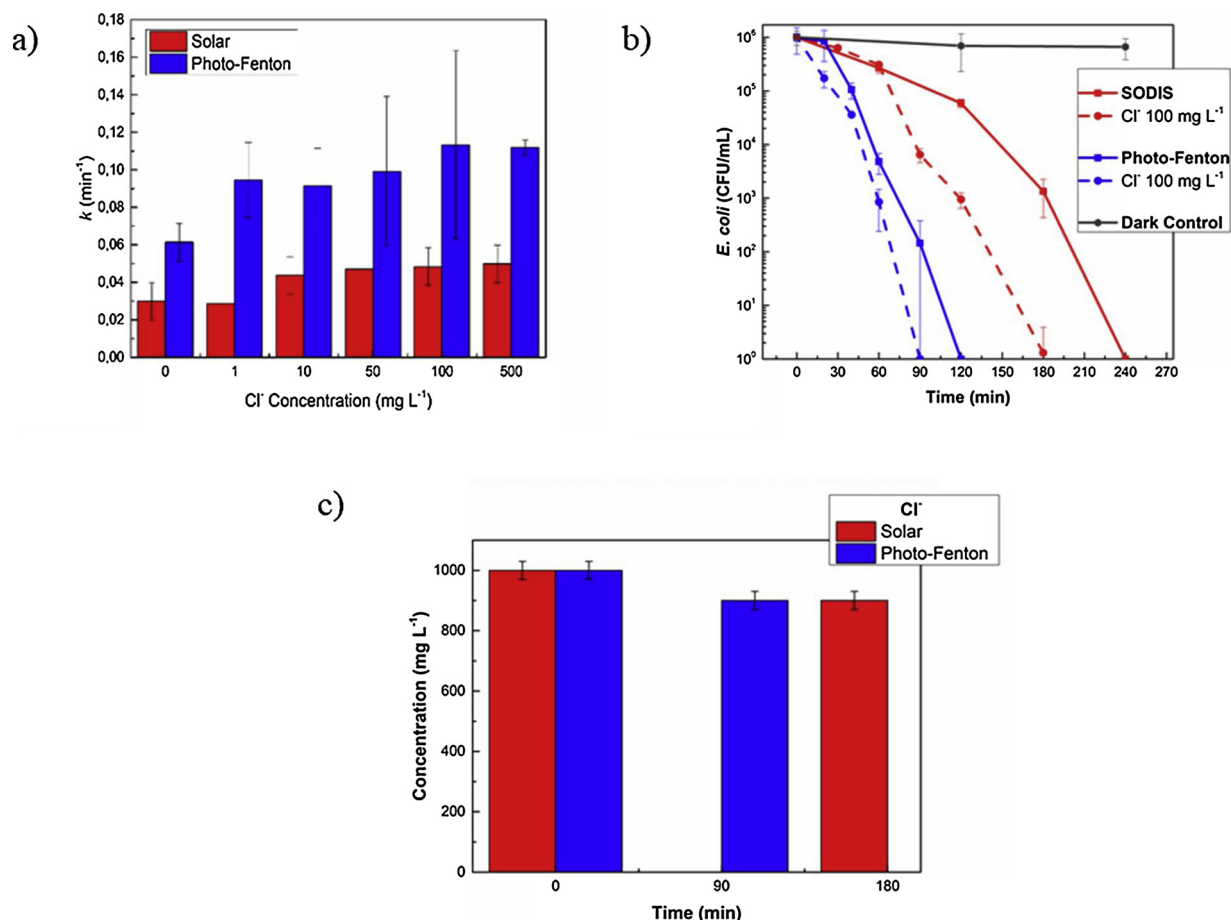


Fig. 2. Kinetic constant values at different Cl⁻ concentrations, for both SODIS and photo-Fenton processes (a). Disinfection experiments with Cl⁻ (b). Changes of Cl⁻ concentration during both processes (c). The detailed disinfection results for SODIS and photo-Fenton in the presence of Cl⁻ are presented in Fig. S2.

CO₃²⁻ has proven germicidal activity [68–70].

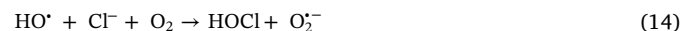
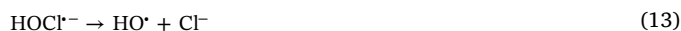
3.1.2. Cl⁻ effects

Fig. 2 summarizes the disinfection experiments that took place in the presence of variable Cl⁻ concentrations. Fig. 2(a) shows the pseudo-first order kinetic constant values calculated for both SODIS and photo-Fenton at all the tested Cl⁻ concentrations, while Fig. 2(b) shows the most significant disinfection graphs. Interestingly, the addition of chloride enhanced disinfection in both cases (SODIS and photo-Fenton), although most likely for different reasons. The pH of both reaction systems was near-neutral, and it showed no substantial shift during either SODIS or photo-Fenton treatments, compared to the experiments in the absence of Cl⁻. A decrease in Cl⁻ concentration during both processes was observed, as shown in Fig. 2(c).

As far as the disinfection enhancement observed during SODIS is concerned, there are a couple of instances in the literature that report a similar phenomenon. The effect is most likely correlated with the membrane-Cl⁻ interactions, which are hypothesized to increase membrane permeability [37,71]. In contrast, in order to explain the increase in efficiency during the photo-Fenton process, one should consider that the interaction between Cl⁻ and Fe³⁺ yields the Fe(Cl)²⁺ and FeCl₂⁺ complexes. In the presence of Cl⁻, Fe(OH)₂²⁺ is replaced by Fe(Cl)²⁺ that has higher absorption coefficient and higher quantum yield of UV photolysis. Photolysis of Fe(Cl)²⁺ promotes the formation of Cl[•] via Eqs. 10–11 [72]. The higher photoactivity of Fe(Cl)²⁺ compared to Fe(OH)₂²⁺ can explain the enhancement of photo-Fenton by chloride (Eqs 10–11).



It is noteworthy that the reaction between Cl⁻ and HO[•], although fast, results in the scavenging of the radical species at acidic pH only, in which case HOCl⁻ is formed that promotes Cl[•] production. However, under neutral to basic conditions HOCl⁻ is effectively decomposed back into Cl⁻ + HO[•], with no net HO[•] scavenging (Eqs. 12–15) [31].



Other possible Cl[•] and HOCl⁻ reactions are presented below: they involve oxidation of Fe²⁺ or reaction with Cl⁻ to form the dichloride radical anions (Cl₂^{•-}) [22,29,73] (Eqs. 16–23). Under near-neutral conditions these reactions would involve Cl[•] produced by FeCl²⁺ photolysis, because at these pH values the reaction between HO[•] and Cl⁻ is not a net Cl[•] source.





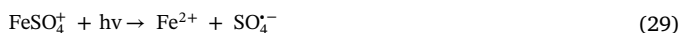
Lastly, termination reactions can lead to the formation of free chlorine that actively participates in the disinfection process (Eqs. 24–26). Moreover, it can explain the decrease of Cl^- observed during the photo-Fenton process. Other termination reactions include the Cl^- recombination or the HOCl reaction with H_2O_2 [29] (Eqs. 27–28).



3.1.3. SO_4^{2-} effects

Fig. 3 summarizes the experimental findings of the bacterial inactivation tests carried out upon addition of sulfate. Fig. 3(a) shows the pseudo-first order kinetic constant values calculated for both SODIS and photo-Fenton processes at all tested SO_4^{2-} concentrations, while Fig. 3(b) reports the most significant disinfection graphs. The obtained results suggest that there are no significant changes in the SODIS reaction kinetics, regardless the SO_4^{2-} concentration added in the 0–500 mg L^{-1} range. In the case of photo-Fenton, a small increase in the inactivation rate was observed. In addition, both pH and SO_4^{2-} concentration showed no substantial changes during either SODIS or photo-Fenton (data not shown).

While in SODIS the effect of sulfates is almost negligible, in the photo-Fenton process the complexation between Fe(III) and SO_4^{2-} yields the species FeSO_4^+ that can produce the sulfate radical, $\text{SO}_4^{\cdot-}$, upon photolysis [21] (Eq. 29).



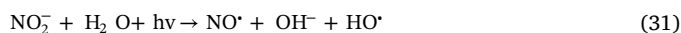
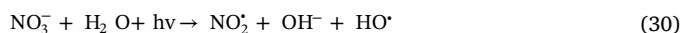
Note that SO_4^{2-} is unable to carry out HO^\cdot scavenging, which can only take place in the presence of HSO_4^- ($\text{pK}_a \sim 2$, which means that the scavenging process can become significant at $\text{pH} < 3$). The radical $\text{SO}_4^{\cdot-}$ is more selective than HO^\cdot , but it can efficiently result in bacterial, viral and chemical contaminant degradation [7,13,42,74,75]. While acting as an oxidant, $\text{SO}_4^{\cdot-}$ yields back SO_4^{2-} . This phenomenon explains why the sulfate concentration did not vary during the photo-Fenton process.

3.1.4. NO_3^- and NO_2^- effects

Fig. 4 gives an overview of the experiments carried out with NO_3^- and NO_2^- . Panels 4(a) and (b) show the pseudo-first order kinetic constant values calculated for both SODIS and photo-Fenton processes, at all tested NO_3^- and NO_2^- concentrations. The most significant disinfection graphs for both processes are reported in Fig. 4(c). In all the cases

the disinfection kinetics was enhanced at all tested concentrations of NO_3^- and NO_2^- , and the effect was higher for NO_2^- compared to NO_3^- . In fact, there is almost a 10-fold difference in the concentrations of NO_3^- that induce a similar enhancement as NO_2^- in bacterial inactivation. This finding is in good agreement with the reported literature data, showing almost 10-fold higher HO^\cdot production by NO_2^- compared to NO_3^- at equal concentration values [76].

It is interesting to observe that the photochemical production of HO^\cdot by nitrate and nitrite has the potential to both shorten the lag time and accelerate the disinfection kinetics in the post-lag, exponential phase (Fig. 4(c)). This finding is in agreement with literature reports, according to which HO^\cdot is one of the transient species involved in post-lag bacterial inactivation and, at the same time, a major actor in inducing cell-membrane damage that exposes the cell to the action of oxidants. Therefore, elevated HO^\cdot causes the lag time to become shorter [47,60]. However, it should be considered that nitrite is a HO^\cdot sink as well as a source [77], and this fact may have interesting implications for the inactivation process (*vide infra*) (Eqs. 30–31).



Generally, NO_3^- and NO_2^- are naturally occurring ions that are part of the nitrogen cycle. These ions can reach both surface water and groundwater because of agricultural activity: in fact, fertilizers contain inorganic nitrogen and wastes contain organic nitrogen, which is first decomposed to give ammonia and then oxidized to give NO_2^- and, finally NO_3^- . It is not surprising that NO_3^- and NO_2^- play a significant role in photochemical processes, although their significance in the photo-Fenton process has been questioned [73]. Our findings suggest that NO_3^- and NO_2^- at environmental concentrations have a real potential to enhance bacterial disinfection, even under photo-Fenton conditions.

3.1.5. NH_4^+ effects

Ammonia is a common, naturally occurring substance. The main local problem of NH_3 released into the air is the unpleasant odor, which is detectable even at low concentrations. The harm caused by NH_4^+ in water bodies is more serious, because it is very toxic to aquatic organisms. Fig. 5 summarizes the experiments carried out upon addition of ammonium sulfate, to simulate an excess of NH_4^+ in water. The sulfate counter-ion was chosen because of its limited effects on bacterial disinfection (see Section 3.3). Fig. 5(a) reports the pseudo-first order kinetic constant values calculated for both SODIS and the photo-Fenton processes at all tested NH_4^+ concentrations, while Fig. 5(b) shows the most significant disinfection graphs. The addition of NH_4^+ had practically no effect in the case of SODIS, while a significant enhancement could be seen with photo-Fenton. The pH of both systems, which is affected by the initial NH_4^+ concentration used, did not show any particular change during either process (Fig. 5c). Furthermore, as shown in

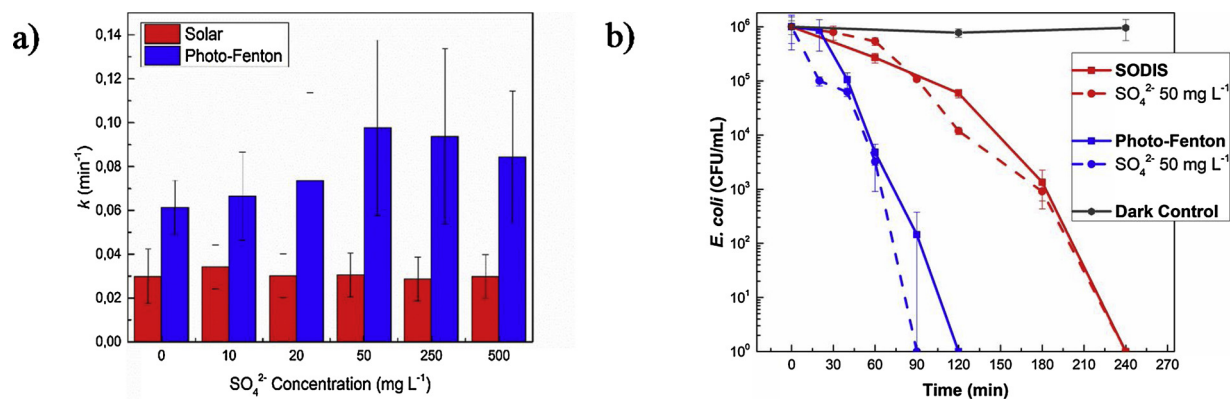


Fig. 3. Kinetic constants values at different SO_4^{2-} concentrations for SODIS and photo-Fenton processes (a). Disinfection experiments with SO_4^{2-} (b). The detailed disinfection results for SODIS and photo-Fenton in the presence of SO_4^{2-} are presented in Fig. S3.

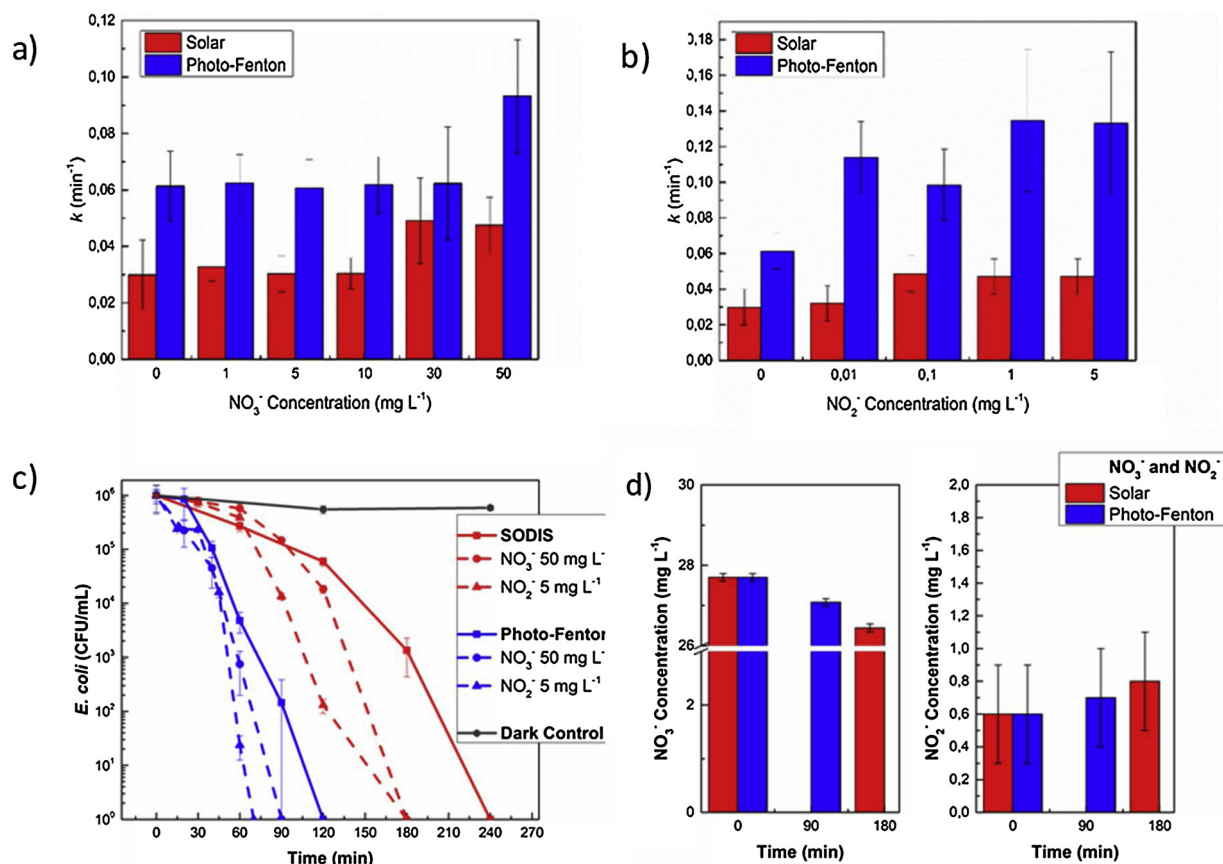
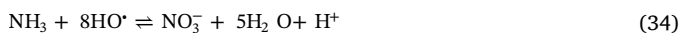
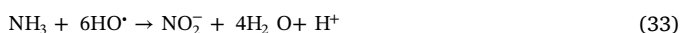


Fig. 4. Kinetic constant values obtained with different NO_3^- (a) and NO_2^- (b) concentrations for SODIS and photo-Fenton processes. Disinfection experiments with NO_3^- and NO_2^- (c). Changes of concentrations during the different processes (d). The detailed disinfection results for SODIS and photo-Fenton in the presence of NO_3^- and NO_2^- are presented in Figs. S4 and S5.

Fig. 5(c), no variation of NH_4^+ concentration was observed during SODIS treatment.

However, the photo-Fenton process revealed a decrease in NH_4^+ concentration (Fig. 5c). The most likely explanation for this finding is that ammonia photo-oxidation by HO^\bullet generates NO_2^- and NO_3^- ions [78,79]. In a summarized way, the reaction pathway reads as follows (Eqs. 32–34):



We note here that although the oxidation of ammonia may be mediated by O_2 , the relevant reaction rates would be very slow [32]. The formation of photochemically active nitrate and nitrite upon ammonia oxidation might explain the observed disinfection enhancement, which is likely due to the production of HO^\bullet upon photolysis of NO_2^- and NO_3^- . The contribution of the SO_4^{2-} counter-ion to bacterial disinfection at the used concentration values of $(\text{NH}_4)_2\text{SO}_4$ is negligible (see Fig. 3).

3.2. Effect of ions on SODIS and photo-Fenton in the presence of Natural Organic Matter (NOM)

The presence of Natural Organic Matter (NOM) in water is ubiquitous, and it is the product of both autochthonous and allochthonous processes [80,81]. NOM can act as a filter for sunlight and, because it absorbs throughout the UV–vis spectrum, it can inhibit the inactivation of *E. coli*. However, UV light absorption by NOM produces the corresponding triplet states ($^3\text{NOM}^*$), the deactivation of which occurs in several ways that include the reaction with oxygen to form singlet

oxygen (see Eqs. 35 and 36). The photoinduced formation of transient species as a function of NOM type, oxygen and NOM concentration was recently systematically investigated, and the main pathways are as follows [45,47] (Eqs. 35–36):



Singlet oxygen can react with water contaminants or bacteria forming peroxidation products, thereby contributing to photochemical decontamination. In addition, if both iron and NOM occur in water at the same time, complex species like $[\text{Fe-NOM}]$ are generated. Compared to NOM, these complexes show higher light absorption and quantum yields, enabling ligand-to-metal charge transfer as shown in Eq. 37. These reactions contribute to bacteria inactivation [82].



Figs. 6 and 7 present an overview of the experimental results obtained when concentrations of ions showing a significant (either positive or negative) effect on disinfection ("optimal" concentrations, as determined in the previous section) were added in the presence or absence of organic matter, for both SODIS (Fig. 6) and photo-Fenton processes (Fig. 7). In both series of experiments, the Suwanee River NOM (SRNOM, 2 mg L^{-1}) that was used as model is expected to actively participate in *E. coli* inactivation. During SODIS a fraction of light can be filtered by SRNOM, inducing its excitation and transient species generation. If the SRNOM amount is sufficiently low and water is not deep (i.e., the optical path is short, as in the present case), the overall system is optically thin and there is limited competition for irradiance between SRNOM and bacteria. Indeed, the fact that bacterial

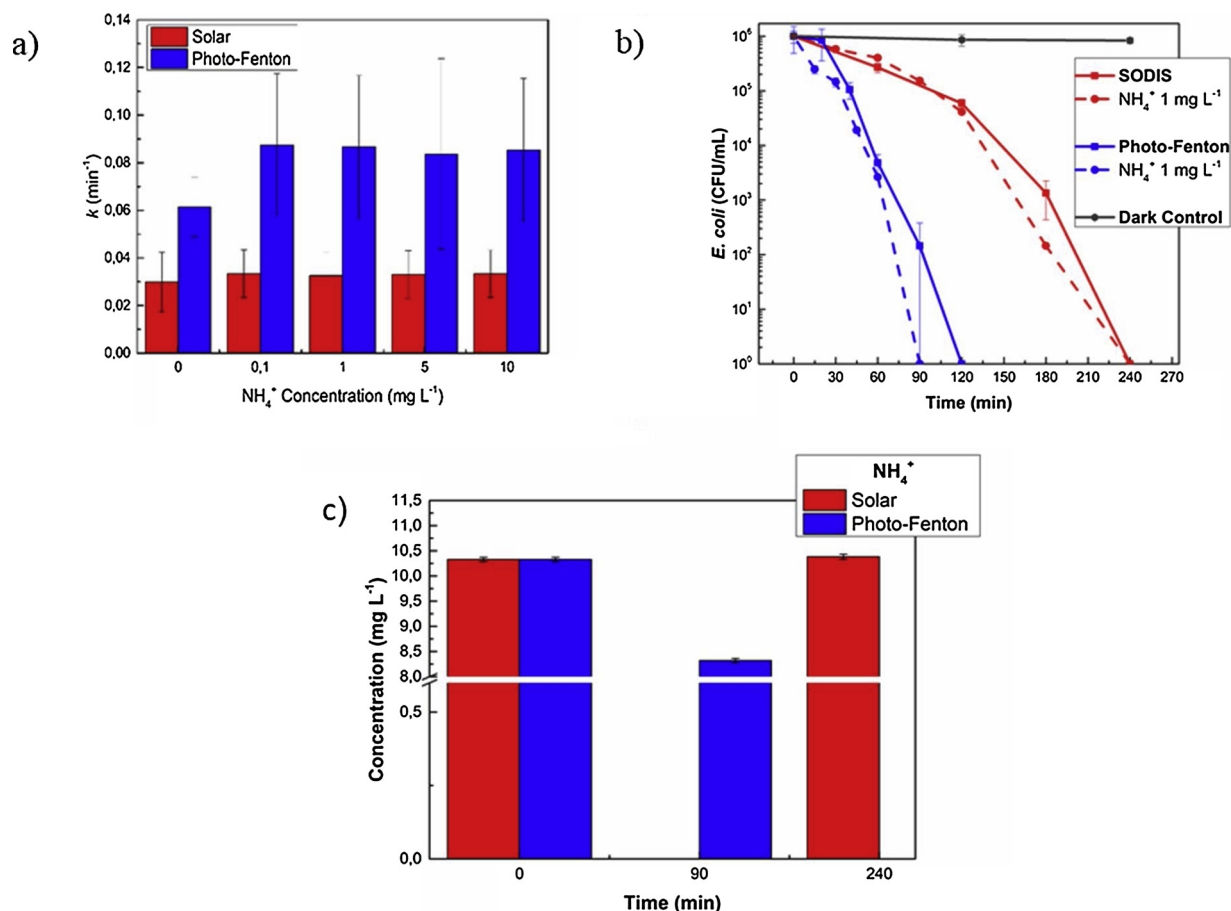


Fig. 5. Kinetic constants values at different NH_4^+ concentrations for SODIS and photo-Fenton processes (a). Disinfection experiments with NH_4^+ (b). Changes of NH_4^+ concentration during the different processes (c). The detailed disinfection results for SODIS and photo-Fenton in the presence of NH_4^+ are presented in Fig. S6.

inactivation showed an increase in kinetics in the presence of the organic material suggests that the photosensitization effect of SRNOM was more important than its light-screening role.

Interestingly, whichever the added ions, no process was significantly faster than plain solar/NOM. Most of the ions did not induce further effects, including NO_3^- , Cl^- , SO_4^{2-} and NH_4^+ . A small but measurable inactivation increase was only observed for NO_2^- (see Section 4.1 for a discussion of this effect), and a notable decrease was attained upon addition of HCO_3^- . The inhibition effect carried out by HCO_3^- could be due to a possible scavenging of the transient species (e.g., $^3\text{NOM}^*$) by HCO_3^- , with possible production of $\text{CO}_3^{\cdot-}$ that may be less reactive compared to $^3\text{NOM}^*$. Actually, $\text{CO}_3^{\cdot-}$ is effectively scavenged by ground-state NOM, differently from $^3\text{NOM}^*$ that mainly reacts with dissolved oxygen [50]; moreover, the interaction between $^3\text{NOM}^*$ and HCO_3^- may partially proceed via physical quenching, without generation of $\text{CO}_3^{\cdot-}$.

The photo-Fenton process was affected by the presence of organic matter in a similar way as SODIS. Firstly, Fe-NOM complexes could be formed in NOM-added photo-Fenton systems; their photolysis enhances the $\text{Fe}^{3+}/\text{Fe}^{2+}$ recycling and, consequently, the disinfection kinetics as well. NOM is able to scavenge all radicals studied before, namely $\text{CO}_3^{\cdot-}$, $\text{SO}_4^{\cdot-}$ and HO^{\cdot} , with high second-order reaction rate constants (in the order of $10^8 \text{ M}^{-1} \text{ s}^{-1}$ for HO^{\cdot} , $10^7 \text{ M}^{-1} \text{ s}^{-1}$ for $\text{SO}_4^{\cdot-}$, and $10^4 \text{ M}^{-1} \text{ s}^{-1}$ for $\text{CO}_3^{\cdot-}$ [69,83–86]). Since there is no correlation between the above scavenging rate constants and the observed effect on bacteria, we can assume that the enhanced formation of reactive species triggered by irradiated NOM and [Fe-NOM] complexes would out-compete the consumption of photogenerated radical transients.

On the contrary, NOM and NO_2^- together increased the photo-Fenton efficiency. However, if we compare the kinetic constants in the

presence of only NOM ($k_1 = 0.1 \text{ min}^{-1}$) and only NO_2^- ($k_2 = 0.13 \text{ min}^{-1}$), with that observed in the simultaneous presence of NOM and NO_2^- ($k_{1,2} = 0.15 \text{ min}^{-1}$), the effect in the mixture is apparently not additive. This result is likely accounted for by the fact that NOM may scavenge part of the HO^{\cdot} radicals photogenerated by NO_2^- .

As a provisional conclusion based on the above findings, we can report that, with minor exceptions, SODIS and photo-Fenton can proceed faster in the presence of organic matter and relatively high amounts of ions. In an effort to generalize our findings about SODIS and photo-Fenton disinfection, the influence of ions and organic matter will be now qualitatively and quantitatively analyzed, regarding the aspects of durability of SODIS and photo-Fenton in the presence/absence of ions, the kinetic modeling of bacterial inactivation (with the aid of APEX software) and the intracellular vs. extracellular pathways to inactivation.

3.3. Vulnerability of SODIS vs. photo-Fenton to the occurrence of ions in water: comparison of time for 4 logU reduction ($T_{99,99\%}$)

In the previous sections, the effects of each ion during SODIS and photo-Fenton were considered. Over the range of concentrations that are expected to be found in natural waters subjected to SODIS, most of the ions showed a variation in their profile of enhancement or antagonism towards the treatment process. If one considers the two disinfection options, namely SODIS and photo-Fenton, for waters with an unknown ionic composition, a valid question would be: which process is safer to be applied as a function of its vulnerability to ions that may be present in water? In order to answer this question, a common response variable was chosen for both processes and all ions, i.e., the time necessary to achieve 4logU reduction ($T_{99,99\%}$) of the bacteria. The

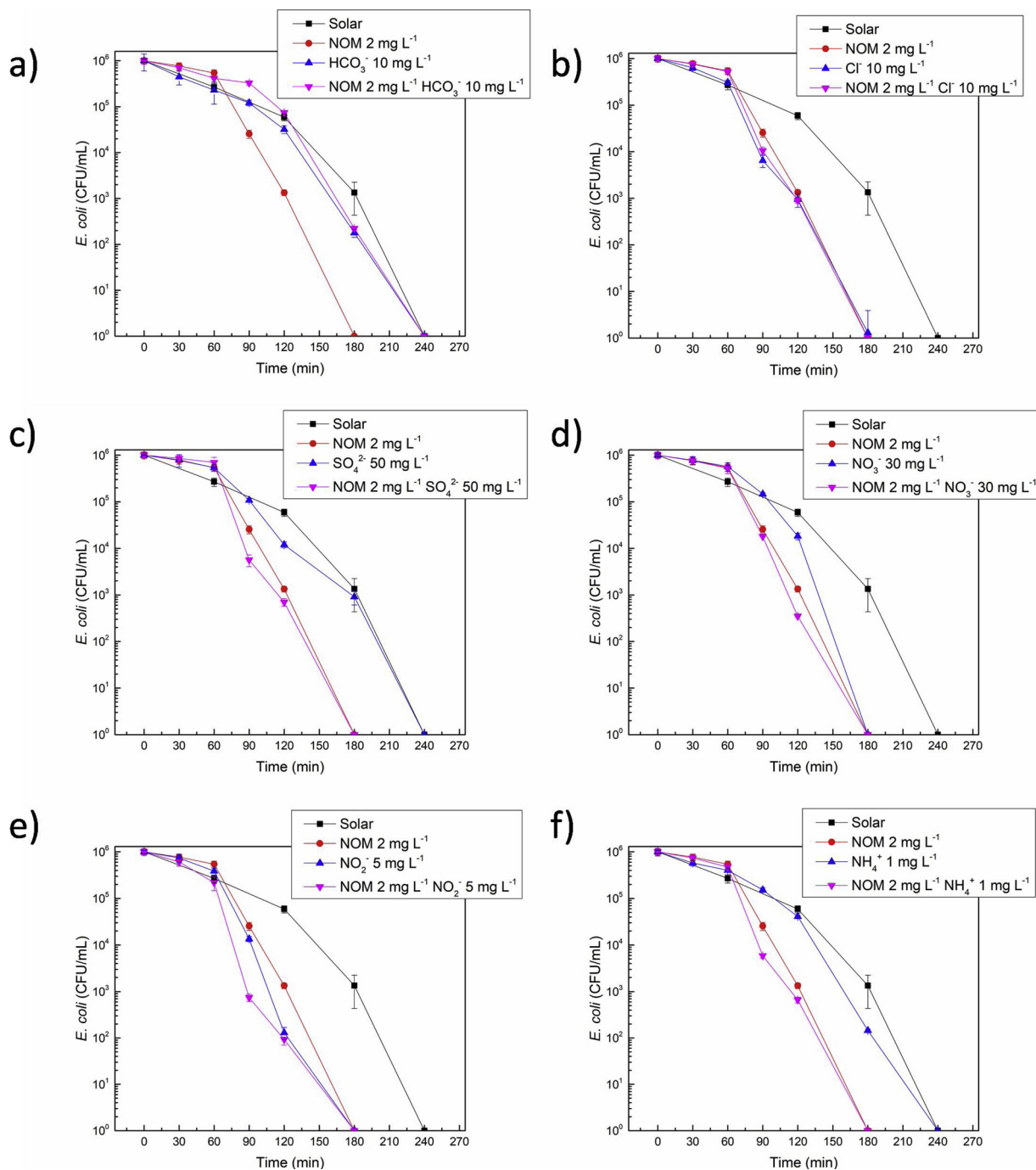


Fig. 6. Combined effect of each studied ion with NOM in SODIS treatment.

results are summarized in Fig. 8.

Fig. 8 presents the change of $T_{99,99\%}$ over the original value achieved by SODIS or photo-Fenton without ions (i.e., 204 and 88 min, respectively: the original 4-logU times can be found in the supplementary material, Table S1). This normalized change was calculated separately for each process and for each anion (Eq. 38):

$$100 \times \left(1 - \frac{T_{99,99\%} - T'_{99,99\%}}{T_{99,99\%}} \right) \quad (38)$$

Where, for each process, $T_{99,99\%}$ was the time necessary for 4 logU reduction and $T'_{99,99\%}$ the corresponding time resulting from the addition of ions.

It can be easily deduced that as an overall trend, all ions improved both processes (i.e., decreased their normalized $T_{99,99\%}$), except for

HCO_3^- during photo-Fenton. As far as the two processes are compared, some ions seem to affect SODIS to a higher extent, namely Cl^- , SO_4^{2-} (at very low concentrations), NO_3^- and NO_2^- . In contrast, NH_4^+ and SO_4^{2-} (at normal/high concentrations) and HCO_3^- rather affect photo-Fenton. A qualitative comparison is given in Table S2. Four of the tested ions acted beneficially for SODIS and photo-Fenton, and two hindered the process; only SO_4^{2-} and Cl^- presented a shift in their influence. Therefore, we can suggest that both SODIS and the photo-Fenton process can work potentially well in natural water, since most of the ions have positive, or at least not negative, effect within their typical concentration ranges. Moreover, the ions show predictable behavior as a function of their concentration in water. Among the types of water that can be used for drinking purposes, groundwater usually has the highest number and concentration of ionic species, as well as higher pH

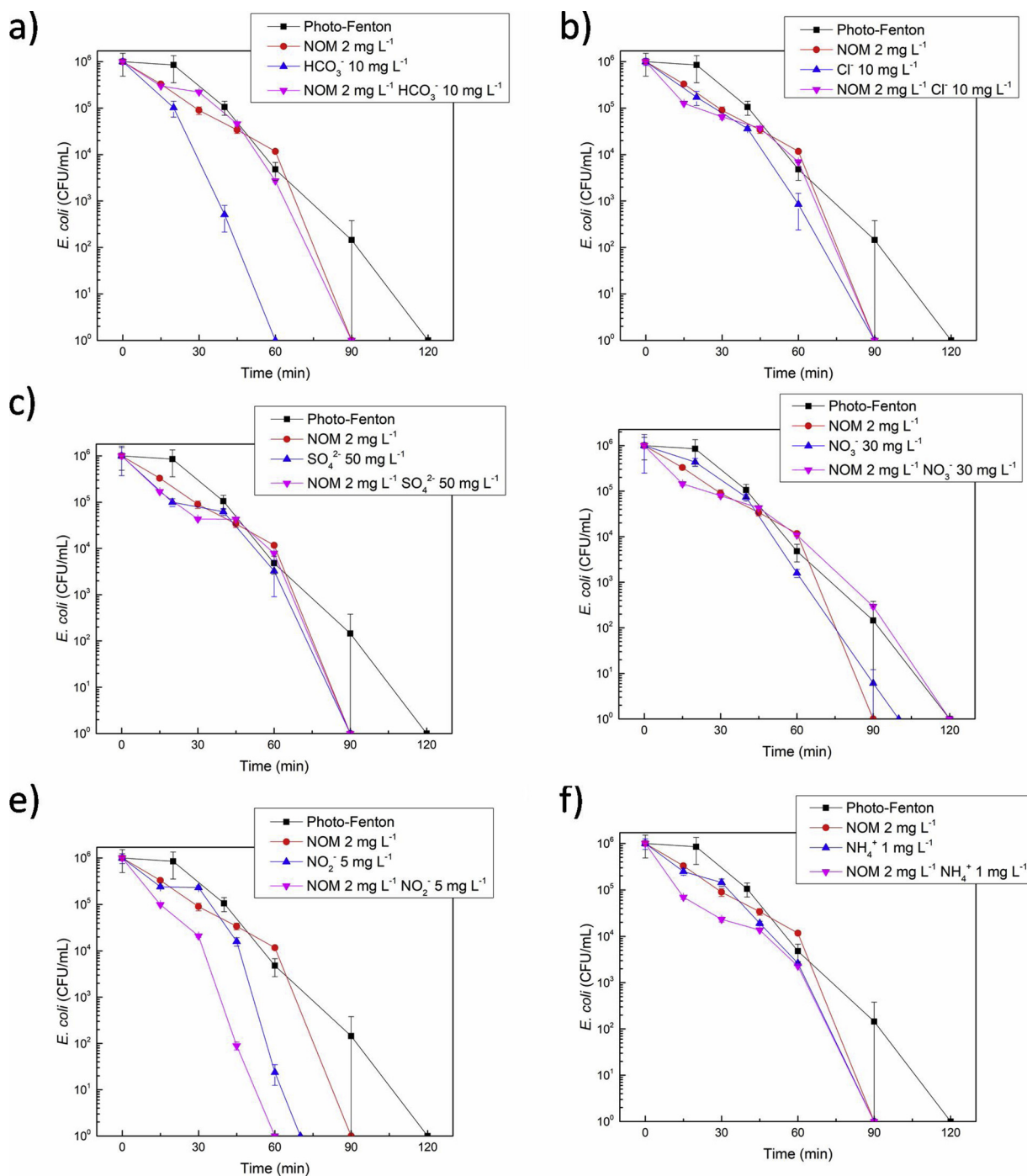


Fig. 7. Combined effect of each studied ion with NOM in photo-Fenton process.

(alkaline).

However, as Fig. 8 suggests, when Cl^- , SO_4^{2-} and NH_4^+ are already encountered at high concentrations, they can have negative (antagonistic) effects during SODIS or photo-Fenton if their concentration is further increased (note that in most cases, even at high ionic concentrations, the treatment was still faster compared to the case of ultra-pure water; however, ultra-pure water does not occur in the natural environment). For instance, in the case of SODIS, SO_4^{2-} and HCO_3^- started inhibiting disinfection at respective concentrations above 20 and 100 mg L^{-1} . For natural waters, 20 mg L^{-1} SO_4^{2-} is a relatively low value while 100 mg L^{-1} HCO_3^- is near the upper limit. Hence, SODIS may be accelerated by increasing HCO_3^- levels, when these are in the moderate concentration range, and it may be slowed down by increasing

SO_4^{2-} at its common concentration values (there may be exceptions for groundwater if it contains little SO_4^{2-} , because in that case increasing SO_4^{2-} could rather enhance disinfection).

Similarly, in the photo-Fenton process, one has inhibition in the presence of 10 mg L^{-1} HCO_3^- or higher, and above 100 mg L^{-1} Cl^- . However, 10 mg L^{-1} HCO_3^- is usually near the lower limit, while 100 mg L^{-1} Cl^- is usually higher than the actual values (except for some groundwaters). Therefore, HCO_3^- can be considered as an antagonistic ion and Cl^- as a synergistic one during the photo-Fenton process. This means that, in the typical concentration ranges of the two ions, photo-Fenton is accelerated by increasing Cl^- and slowed down by increasing HCO_3^- . Finally, NO_3^- , NO_2^- and NH_4^+ could be viewed as enhancing factors due to their (low or high) production of HO^\bullet (direct in the case

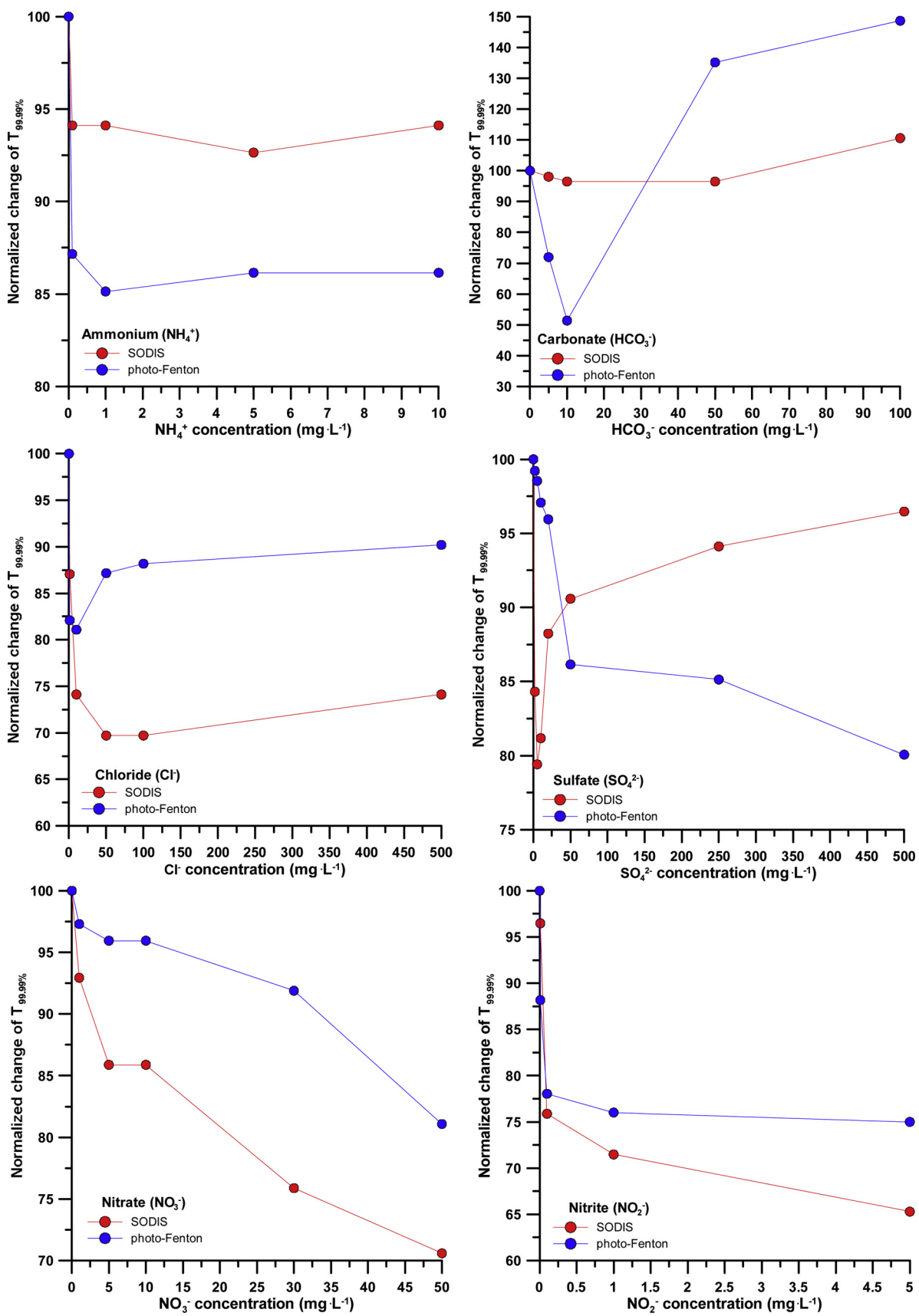


Fig. 8. Normalized changes (%) in the necessary time to remove 4 logU of bacteria in waters containing ions.

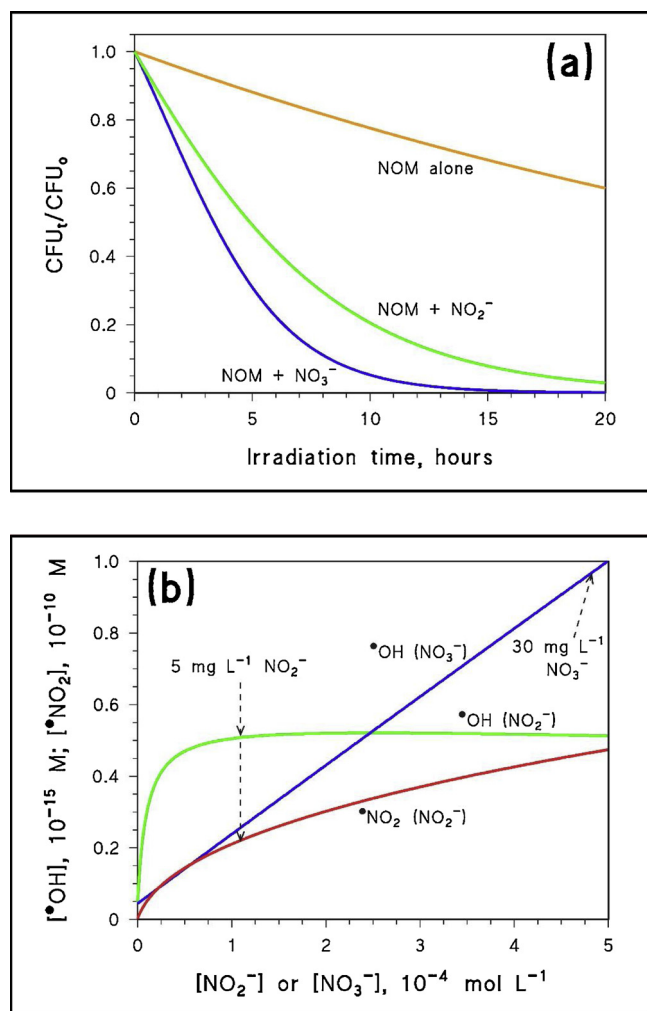


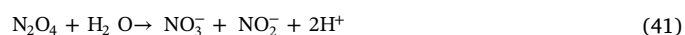
Fig. 9. Modeled trends of exogenous bacterial photoinactivation in the systems containing NOM, NOM + NO_2^- ($NO_2^- = 5 \text{ mg L}^{-1}$) and NOM + NO_3^- ($NO_3^- = 30 \text{ mg L}^{-1}$) (a). Modeled steady-state concentrations of HO^\bullet and NO_2^\bullet , as a function of the concentration values of NO_2^- or NO_3^- (b). In both cases the concentration value of NOM (2 mg L^{-1}) was the same as per the corresponding SODIS experiments described in Fig. 6. Model sunlight had a UV irradiance (290–400 nm) of 22 W m^{-2} , water depth was 7.5 cm .

of NO_3^- and NO_2^- , indirect -oxidation mediated- in the case of NH_4^+). Besides, the simultaneous presence of ions could impact the expected individual effect, and present antagonism; this explains why many studies in literature encounter a reduction in kinetics when experimenting with natural water sources.

From the previous parts it can be concluded that in the presence of ions in water, bacterial inactivation is highly dependent on their concentration and, most importantly, the process would be mainly governed by events that take place in the solution bulk (as opposed to events affecting the bacterial cells or membranes). As such, an attempt to model the bacterial inactivation by solar-mediated processes could be performed with the APEX software. The SODIS systems containing NOM, NOM + NO_2^- and NOM + NO_3^- are amenable to photochemical modeling, as far as endogenous inactivation alone is concerned. The model predicts considerably slower kinetics compared to laboratory experiments (compare the model trends of Fig. 9a with the experimental trends for comparable systems, reported in Fig. 6), for several reasons that are listed in Section 2.5. However, the relative kinetics (i.e., what is faster and what is slower) should be preserved despite these differences [60]. In this context, it is interesting to observe that the model results in Fig. 9a predict the NOM + NO_3^- system to produce

faster inactivation compared to NOM + NO_2^- , in clear disagreement with the experimental data. The reason is that the steady-state $[HO^\bullet]$ would be higher in the presence of 30 mg L^{-1} nitrate compared to 5 mg L^{-1} nitrite, as shown in Fig. 9b. Indeed, although NO_2^- is more photoactive than NO_3^- and undergoes photolysis to a higher extent (the HO^\bullet formation rate is predicted to be higher with 5 mg L^{-1} NO_2^- than with 30 mg L^{-1} NO_3^-), NO_2^- itself also acts as HO^\bullet scavenger. Indeed, in the presence of 5 mg L^{-1} NO_2^- and 2 mg L^{-1} NOM, NO_2^- scavenges around 90 % of the HO^\bullet it mostly contributes to photo-generate (in such conditions, NO_2^- photolysis would produce 99.5 % of HO^\bullet , the remainder being generated by NOM). The HO^\bullet scavenging by NO_2^- accounts for the plateau in the relevant $[HO^\bullet]$ curve of Fig. 9b, while no plateau is observed in the case of nitrate.

However, the reaction between HO^\bullet and NO_2^- yields a further transient species (NO_2^\bullet) that might also be involved in the bacterial inactivation process [77]:



Considering the kinetic system made up of reactions [39–41], and applying the steady-state approximation to HO^\bullet , NO_2^\bullet and N_2O_4 , one gets the following expression for the steady-state $[NO_2^\bullet]$ (where k_{40} is the rate constant of $2NO_2^\bullet \rightarrow N_2O_4$, and k_{41} is the rate constant of $N_2O_4 \rightarrow 2NO_2^-$) [77]:

$$[NO_2^\bullet] = \sqrt{\frac{k_{40} + k_{41}}{k_{39} \cdot 2k_{40}k_{41}}} [HO^\bullet][NO_2^-] = \sqrt{88} [HO^\bullet][NO_2^-] \quad (42)$$

Eq. (42) was used to model $[NO_2^\bullet]$ in Fig. 9b, showing a continuous increase with increasing $[NO_2^-]$. NO_2^\bullet is much less reactive than HO^\bullet , but it is predicted to be five orders of magnitude more concentrated. Therefore, there is potential for NO_2^\bullet to contribute to *E. coli* inactivation, which could explain why the nitrite-containing system was more effective than the nitrate one, despite the lower predicted $[HO^\bullet]$.

3.4. Extracellular vs. Intracellular mechanisms of bacterial inactivation during SODIS and photo-Fenton processes

In many of the processes considered so far, bacteria are the terminal acceptor (target) of a transient species that leads to their inactivation. The addition of ions in the bulk suggests that the participation of the transient species to photo-chemical events happens in the bulk as well. With a few possible exceptions, the short lifetimes of the transients suggest that the occurring damage is located at the cell wall, whose eventual rupture leads to bacterial death. However, there is growing evidence that bacterial inactivation by the photo-Fenton or the persulfate process can also affect the intracellular domain of microorganisms [15,74]. Here we present an overview of the pathways that are induced when certain ions are present in the extracellular environment of bacteria, and how their presence might affect bacterial inactivation mechanisms.

Among the mentioned ions, NO_3^- / NO_2^- , SO_4^{2-} and HCO_3^- can interfere with the “normal” disinfection events that take place in pure water. Firstly, in the anaerobic metabolism, NO_3^- / NO_2^- mediate cellular respiration and become electron acceptors. Even in aerobic conditions, during assimilatory metabolism, NO_3^- and NO_2^- can be imported into the cell by the *Nrt* family of transporters (NRT-nitrate transporters). Nitrate is then reduced to NO_2^- by *Nar* (Nar-nitrate reductases), and it follows final conversion to NH_3 [87] (see the Kyoto Encyclopedia of Genes and Genomes -KEGG pathway extract in the supplementary material, Fig. S7). Also, sulfur is essential to *E. coli* for cysteine synthesis, thus there is an active system of SO_4^{2-} transport into the cell (3.4 mgS/mL cells) by sulfate transporters (Cys-sulfate permease family) [88,89] (see KEGG pathway in the supplementary material, Fig. S8). HCO_3^- can also be

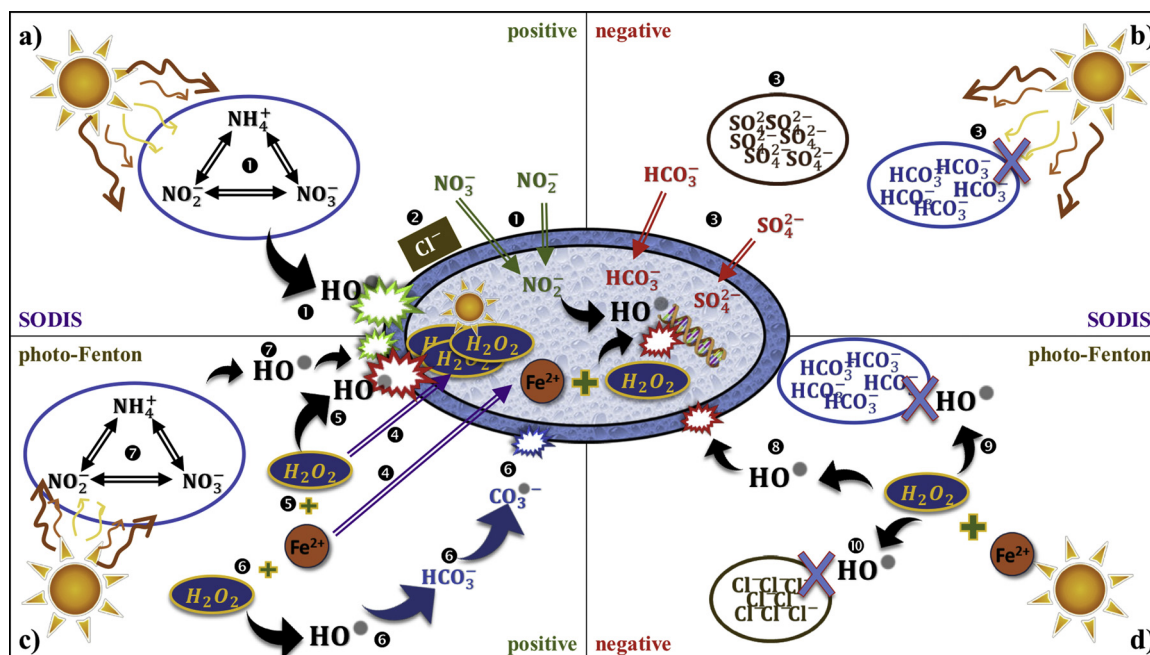


Fig. 10. Overall mechanistic proposition for the influence of ions on bacterial inactivation.

transferred by the bicarbonate transporters family or the *Sbt* (Sbt-sodium-dependent bicarbonate transporter) homologues [90] (see a summary of the transporters in supplementary Fig. S8).

If we account for the photo-Fenton process taking place inside the cell, (and involving "natural" intracellular, non-bulk added, Fe and H_2O_2), which also leads to the generation of HO^\bullet , then the aforementioned ions at high concentration may cause a new intracellular oxidative balance: NO_3^-/NO_2^- upon irradiation may yield further intracellular HO^\bullet , while HCO_3^- might scavenge the generated HO^\bullet to produce CO_3^{2-} and SO_4^{2-} might complex Fe^{3+} . As such, a summary of the intracellular and extracellular mechanisms that lead to bacterial inactivation is provided in Fig. 10.

The depicted actions are separated horizontally as SODIS (10a,b) and photo-Fenton (10c,d) while their effect, positive or negative is denoted vertically (positive: 10a,c and negative: 10b,d). The overview of the involved actions is as follows, stating from SODIS (numbers below correspond to those in Fig. 10):

Action 1: Light-mediated excitation of NO_3^-/NO_2^- leads to the generation of HO^\bullet (Fig. S10). Moreover, the occurrence of NO_3^-/NO_2^- in the bulk suggests their possible transport into the intracellular domain, where they could generate further HO^\bullet . **Action 2:** Cl^- affects the bacterial membrane by reducing its viability. **Action 3:** On the other hand, the presence of high amounts of HCO_3^- inhibits SODIS and, in addition to the bulk effects of HCO_3^- , this ion may affect intracellular inactivation as well. For instance, high intracellular HCO_3^- may act as an important HO^\bullet scavenger and inhibit the internal (SODIS-triggered) photo-Fenton reactions (the latter would involve the Fe species and H_2O_2 that naturally occur in the intra-cellular compartments, even without external addition of Fenton reagents [15]).

For the photo-Fenton process, the following actions can be highlighted. **Action 4:** The presence of Fe^{2+} and H_2O_2 in the solution ensures the transport of both species into the cell and, consequently, the enhancement of intracellular photo-Fenton. **Action 5:** The above process (4) leads to the generation of HO^\bullet that attacks the cell, while light regenerates Fe^{3+} to Fe^{2+} . **Action 6:** The HO^\bullet generated as per the above discussion can react with HCO_3^- to produce CO_3^{2-} . **Action 7:** Furthermore, in the presence of NO_3^-/NO_2^- , additional HO^\bullet production ensues that enhances bacterial inactivation. On the other hand, the normal HO^\bullet production (**Action 8**) is disrupted by high amounts of

HCO_3^- that acts as scavenger, thereby exerting a negative effect on both the HO^\bullet occurrence (**Action 9** and **Action 10**) and the subsequent bacterial inactivation.

4. Conclusions

In this work, the effect of inorganic ions and natural organic matter occurring in aqueous matrices on the efficacy of *E. coli* removal by the SODIS and photo-Fenton processes was systematically studied. The investigated concentration values varied extensively to cover commonly encountered concentrations in surface waters, rainwater and groundwater, which constitute the most commonly used matrices in solar-mediated disinfection.

From the obtained results, we can confer that not all ions have the same impact, and their effect is subject to the concentration values and the process applied (SODIS or photo-Fenton). More specifically, HCO_3^- was found to produce a small enhancement in inactivation kinetics in some conditions but, at environmentally relevant concentrations, it will always be an antagonistic factor. On the contrary, NO_3^-/NO_2^- and NH_4^+ , can be expected to aid either SODIS or photo-Fenton disinfection. Disinfection by both processes will be faster in the presence of Cl^- and SO_4^{2-} than in their absence but, starting from the typical concentration values found in surface waters, a further increase of Cl^- will enhance SODIS while disrupting the photo-Fenton process, and the opposite will occur with SO_4^{2-} . Nevertheless, despite the various levels tested in this study, natural waters that contain a mixture of these ions and NOM present in various cases a negative impact. Furthermore, although NOM was beneficial for both SODIS and photo-Fenton, its presence can be an inhibiting factor for the secondary oxidants and radicals generated by the ionic species during the photo-assisted processes (except for NO_2^-). However, a wider investigation will be necessary to locate the possible tipping point(s) in the interaction between NOM and the ions.

Finally, from the aforementioned results we can conclude that SODIS and photo-Fenton are quite robust processes: they are certainly suitable for the disinfection of natural waters, although their effectiveness could be hampered when treating some types of groundwater. Indeed, in most cases the added ions at typical concentration values in surface waters produced a decrease in the time required to inactivate 99.99 % of *E. coli* (exception: HCO_3^-). In addition, even in highly antagonistic conditions, photo-Fenton was always faster than the SODIS

process. This fact makes photo-Fenton an attractive solution that must be further evaluated in sunny or developing countries, to see whether it really is an effective measure at household or community level to achieve natural water disinfection.

CRedit authorship contribution statement

Elena Rommozzi: Investigation, Writing - original draft, Writing - review & editing, Visualization. **Stefanos Giannakis:** Methodology, Validation, Writing - original draft, Writing - review & editing, Visualization, Project administration, Supervision. **Rita Giovannetti:** Resources, Writing - original draft, Writing - review & editing, Supervision, Funding acquisition. **Davide Vione:** Formal analysis, Investigation, Writing - original draft, Writing - review & editing, Visualization, Project administration. **César Pulgarin:** Resources, Writing - original draft, Writing - review & editing, Project administration, Funding acquisition, Supervision.

Declaration of Competing Interest

The authors declare that they have no known competing financial interests or personal relationships that could have appeared to influence the work reported in this paper.

Acknowledgements

Cesar Pulgarin would like to acknowledge the financial support through the European project WATERSPOUTT H2020-Water-5c-2015 GA 688928 and the Swiss State Secretariat for Education, Research and Innovation SEFRI-WATERSPOUTT, No.: 588141. Stefanos Giannakis acknowledges the Spanish Ministry of Science, Innovation and Universities (MICIU) for the Ramón y Cajal Fellowship (RYC2018-024033-I). Davide Vione acknowledges financial support from University of Torino and Compagnia di San Paolo (project CSTO168282-ABATEPHARM). Finally, Elena Rommozzi and Rita Giovanetti would like to acknowledge the International School of Advanced Studies of Camerino University for the financial support of the research stay of Elena Rommozzi in EPFL.

Appendix A. Supplementary data

Supplementary material related to this article can be found, in the online version, at doi:<https://doi.org/10.1016/j.apcatb.2020.118877>.

References

- [1] M. Boyle, C. Sichel, P. Fernández-Ibáñez, G.B. Arias-Quiroz, M. Iriarte-Puñá, A. Mercado, E. Ubomba-Jaswa, K.G. McGuigan, Bactericidal effect of solar water disinfection under real sunlight conditions, *Appl. Environ. Microbiol.* 74 (2008) 2997–3001, <https://doi.org/10.1128/AEM.02415-07>.
- [2] S. Giannakis, A.I. Merino Gamo, E. Darakas, A. Escalas-Cañellas, C. Pulgarin, Monitoring the post-irradiation *E. coli* survival patterns in environmental water matrices: implications in handling solar disinfected wastewater, *Chem. Eng. J.* 253 (2014), <https://doi.org/10.1016/j.cej.2014.05.092>.
- [3] E. Ubomba-Jaswa, C. Navntoft, M.I. Polo-López, P. Fernandez-Ibáñez, K.G. McGuigan, Solar disinfection of drinking water (SODIS): an investigation of the effect of UV-A dose on inactivation efficiency, *Photochem. Photobiol. Sci.* 8 (2009) 587–595, <https://doi.org/10.1039/b816593a>.
- [4] M. Fisher, C. Keenan, K. Nelson, B. Voelker, Speeding up solar disinfection (SODIS): effects of hydrogen peroxide, temperature, pH, and copper plus ascorbate on the photoinactivation of *E. coli*, *J. Water Health* 6 (2008) 35–51.
- [5] S. Giannakis, E. Darakas, A. Escalas-Cañellas, C. Pulgarin, Temperature-dependent change of light dose effects on *E. coli* inactivation during simulated solar treatment of secondary effluent, *Chem. Eng. Sci.* 126 (2015), <https://doi.org/10.1016/j.ces.2014.12.045>.
- [6] F. Sciacca, J.A. Rengifo-Herrera, J. Wéthé, C. Pulgarin, Dramatic enhancement of solar disinfection (SODIS) of wild *Salmonella* sp. in PET bottles by H₂O₂ addition on natural water of Burkina Faso containing dissolved iron, *Chemosphere* 78 (2010) 1186–1191.
- [7] J. Rodríguez-Chueca, S. Giannakis, M. Marjanovic, M. Kohantorabi, M.R. Gholami, D. Grandjean, L.F. de Alencastro, C. Pulgarin, Solar-assisted bacterial disinfection and removal of contaminants of emerging concern by Fe²⁺-activated HSO₅⁻ vs. S2O8²⁻ in drinking water, *Appl. Catal. B Environ.* 248 (2019) 62–72, <https://doi.org/10.1016/J.APCATB.2019.02.018>.
- [8] E. Ubomba-Jaswa, P. Fernández-Ibáñez, C. Navntoft, M.I. Polo-López, K.G. McGuigan, Investigating the microbial inactivation efficiency of a 25 L batch solar disinfection (SODIS) reactor enhanced with a compound parabolic collector (CPC) for household use, *J. Chem. Technol. Biotechnol.* 85 (2010) 1028–1037.
- [9] S.C. Kehoe, T.M. Joyce, P. Ibrahim, J.B. Gillespie, R.A. Shahar, K.G. McGuigan, Effect of agitation, turbidity, aluminium foil reflectors and container volume on the inactivation efficiency of batch-process solar disinfectors, *Water Res.* 35 (2001) 1061–1065.
- [10] J. Ndounla, C. Pulgarin, Solar light (hv) and H₂O₂/hv photo-disinfection of natural alkaline water (pH 8.6) in a compound parabolic collector at different day periods in Sahelian region, *Environ. Sci. Pollut. Res.* (2015) 1–13, <https://doi.org/10.1007/s11356-015-4784-0>.
- [11] D. Spuhler, J.A. Rengifo-Herrera, C. Pulgarin, The effect of Fe²⁺, Fe³⁺, H₂O₂ and the photo-Fenton reagent at near neutral pH on the solar disinfection (SODIS) at low temperatures of water containing *Escherichia coli* K12, *Appl. Catal. B* 96 (2010) 126–141, <https://doi.org/10.1016/j.apcatb.2010.02.010>.
- [12] S. Giannakis, M.I.P. López, D. Spuhler, J.A.S. Pérez, P.F. Ibáñez, C. Pulgarin, Solar disinfection is an augmentable, in situ-generated photo-Fenton reaction-Part 2: A review of the applications for drinking water and wastewater disinfection, *Appl. Catal. B Environ.* 198 (2016), <https://doi.org/10.1016/j.apcatb.2016.06.007>.
- [13] M. Marjanovic, S. Giannakis, D. Grandjean, L.F. de Alencastro, C. Pulgarin, Effect of MM Fe addition, mild heat and solar UV on sulfate radical-mediated inactivation of bacteria, viruses, and micropollutant degradation in water, *Water Res.* 140 (2018) 220–231, <https://doi.org/10.1016/j.watres.2018.04.054>.
- [14] J.A. Imlay, Diagnosing oxidative stress in bacteria: not as easy as you might think, *Curr. Opin. Microbiol.* 24 (2015) 124–131.
- [15] S. Giannakis, M. Voumard, S. Rtimi, C. Pulgarin, Bacterial disinfection by the photo-Fenton process: Extracellular oxidation or intracellular photo-catalysis? *Appl. Catal. B Environ.* 227 (2018) 285–295, <https://doi.org/10.1016/j.apcatb.2018.01.044>.
- [16] S. Giannakis, C. Ruales-Lonfat, S. Rtimi, S. Thabet, P. Cotton, C. Pulgarin, Castles fall from inside: evidence for dominant internal photo-catalytic mechanisms during treatment of *Saccharomyces cerevisiae* by photo-Fenton at near-neutral pH, *Appl. Catal. B Environ.* 185 (2016), <https://doi.org/10.1016/j.apcatb.2015.12.016>.
- [17] C. Ruales-Lonfat, N. Benítez, A. Sienkiewicz, C. Pulgarin, Deleterious effect of homogeneous and heterogeneous near-neutral photo-Fenton system on *Escherichia coli*. Comparison with photo-catalytic action of TiO₂ during cell envelope disruption, *Appl. Catal. B Environ.* 160 (2014) 286–297.
- [18] S. Giannakis, Analogies and differences among bacterial and viral disinfection by the photo-Fenton process at neutral pH: a mini review, *Environ. Sci. Pollut. Res.* (2018), <https://doi.org/10.1007/s11356-017-0926-x>.
- [19] A.-G. Rincón, C. Pulgarin, Effect of pH, inorganic ions, organic matter and H₂O₂ on *E. coli* K12 photocatalytic inactivation by TiO₂: implications in solar water disinfection, *Appl. Catal. B Environ.* 51 (2004) 283–302.
- [20] P. Villegas-Guzman, F. Hofer, J. Silva-Agredo, R.A. Torres-Palma, Role of sulfate, chloride, and nitrate anions on the degradation of fluoroquinolone antibiotics by photoelectro-Fenton, *Environ. Sci. Pollut. Res.* 24 (2017) 28175–28189.
- [21] A. Machulek Jr., J.E.F. Moraes, L.T. Okano, C.A. Silvério, F.H. Quina, Photolysis of ferric ions in the presence of sulfate or chloride ions: implications for the photo-Fenton process, *Photochem. Photobiol. Sci.* 8 (2009) 985–991.
- [22] J. De Laet, G.T. Le, B. Legube, A comparative study of the effects of chloride, sulfate and nitrate ions on the rates of decomposition of H₂O₂ and organic compounds by Fe(II)/H₂O₂ and Fe(III)/H₂O₂, *Chemosphere* 55 (2004) 715–723.
- [23] A.-G. Rincón, C. Pulgarin, Solar photolytic and photocatalytic disinfection of water at laboratory and field scale. Effect of the chemical composition of water and study of the postirradiation events, *J. Sol. Energy Eng.* 129 (2007) 100–110.
- [24] J. Soler, A. García-Ripoll, N. Hayek, P. Miró, R. Vicente, A. Arques, A.M. Amat, Effect of inorganic ions on the solar detoxification of water polluted with pesticides, *Water Res.* 43 (2009) 4441–4450.
- [25] B.D. McGinnis, V.D. Adams, E.J. Middlebrooks, Degradation of ethylene glycol in photo Fenton systems, *Water Res.* 34 (2000) 2346–2354.
- [26] I. Oller, W. Gernjak, M.I. Maldonado, P. Fernandez-Ibanez, J. Blanco, J.A. Sánchez-Pérez, S. Malato, Degradation of the insecticide dimethoate by solar photocatalysis at pilot plant scale, *Environ. Chem. Lett.* 3 (2005) 118–121.
- [27] S.S. Da Silva, O. Chivavone-Filho, E.L. de Barros Neto, E.L. Foletto, A.L.N. Mota, Effect of inorganic salt mixtures on phenol mineralization by photo-Fenton-analysis via an experimental design, *Water Air Soil Pollut.* 225 (2014) 1784.
- [28] H.M. Gutiérrez-Zapata, K.L. Rojas, J. Sanabria, J.A. Rengifo-Herrera, 2,4-D abatement from groundwater samples by photo-Fenton processes at circumneutral pH using naturally iron present. Effect of inorganic ions, *Environ. Sci. Pollut. Res.* (2016) 1–9, <https://doi.org/10.1007/s11356-016-7067-5>.
- [29] J.E. Grebel, J.J. Pignatello, W.A. Mitch, Effect of halide ions and carbonates on organic contaminant degradation by hydroxyl radical-based advanced oxidation processes in saline waters, *Environ. Sci. Technol.* 44 (2010) 6822–6828.
- [30] J.E. Grebel, J.J. Pignatello, W.A. Mitch, Impact of halide ions on natural organic matter-sensitized photolysis of 17β-estradiol in saline waters, *Environ. Sci. Technol.* 46 (2012) 7128.
- [31] G.G. Jayson, B.J. Parsons, A.J. Swallow, Some simple, highly reactive, inorganic chlorine derivatives in aqueous solution. Their formation using pulses of radiation and their role in the mechanism of the Fricke dosimeter, *J. Chem. Soc. Faraday Trans. 1 Phys. Chem. Condens. Phases* 69 (1973) 1597–1607.
- [32] J.J. Pignatello, E. Oliveros, A. MacKay, Advanced oxidation processes for organic contaminant destruction based on the fenton reaction and related chemistry, *Crit. Rev. Environ. Sci. Technol.* 36 (2006) 1–84, <https://doi.org/10.1080/>

- 10643380500326564.
- [33] K.L. Nelson, A.B. Boehm, R.J. Davies-Colley, M.C. Dodd, T. Kohn, K.G. Linden, Y. Liu, P.A. Maraccini, K. McNeill, W.A. Mitch, Sunlight-mediated inactivation of health-relevant microorganisms in water: a review of mechanisms and modeling approaches, *Environ. Sci. Process. Impacts* 20 (2018) 1089–1122.
- [34] Y. Yang, J.J. Pignatello, J. Ma, W.A. Mitch, Comparison of halide impacts on the efficiency of contaminant degradation by sulfate and hydroxyl radical-based advanced oxidation processes (AOPs), *Environ. Sci. Technol.* 48 (2014) 2344–2351.
- [35] C.-H. Liao, S.-F. Kang, F.-A. Wu, Hydroxyl radical scavenging role of chloride and bicarbonate ions in the H₂O₂/UV process, *Chemosphere*. 44 (2001) 1193–1200, [https://doi.org/10.1016/S0045-6535\(00\)00278-2](https://doi.org/10.1016/S0045-6535(00)00278-2).
- [36] E. Lipczynska-Kochany, G. Sprah, S. Harms, Influence of some groundwater and surface waters constituents on the degradation of 4-chlorophenol by the Fenton reaction, *Chemosphere* 30 (1995) 9–20, [https://doi.org/10.1016/0045-6535\(94\)00371-Z](https://doi.org/10.1016/0045-6535(94)00371-Z).
- [37] A.-G. Rincón, C. Pulgarin, Effect of pH, inorganic ions, organic matter and H₂O₂ on *E. coli* K12 photocatalytic inactivation by TiO₂: implications in solar water disinfection, *Appl. Catal. B Environ.* 51 (2004) 283–302, <https://doi.org/10.1016/j.apcatb.2004.03.007>.
- [38] G.V. Buxton, C.L. Greenstock, W.P. Helman, A.B. Ross, Critical review of rate constants for reactions of hydrated electrons, hydrogen atoms and hydroxyl radicals ($\cdot\text{OH}/\cdot\text{O}$) in aqueous solution, *J. Phys. Chem. Ref. Data* 17 (1988) 513.
- [39] J. Mack, J.R. Bolton, Photochemistry of nitrite and nitrate in aqueous solution: a review, *J. Photochem. Photobiol. A Chem.* 128 (1999) 1, [https://doi.org/10.1016/S1010-6030\(99\)00155-0](https://doi.org/10.1016/S1010-6030(99)00155-0).
- [40] L. Carena, M. Minella, F. Barsotti, M. Brigante, M. Milan, A. Ferrero, S. Berto, C. Minero, D. Vione, Phototransformation of the herbicide propanil in Paddy Field Water, *Environ. Sci. Technol.* 51 (2017) 2695–2704, <https://doi.org/10.1021/acs.est.6b05053>.
- [41] S. Giannakis, M.I. Polo López, D. Spuhler, J.A. Sánchez Pérez, P. Fernández Ibáñez, C. Pulgarin, Solar disinfection is an augmentable, in situ-generated photo-Fenton reaction—part I: a review of the mechanisms and the fundamental aspects of the process, *Appl. Catal. B Environ.* 199 (2016) 199–223, <https://doi.org/10.1016/j.apcatb.2016.06.009>.
- [42] L.G. Devi, C. Munikrishnappa, B. Nagaraj, K.E. Rajashekhar, Effect of chloride and sulfate ions on the advanced photo Fenton and modified photo Fenton degradation process of Alizarin Red S, *J. Mol. Catal. A Chem.* 374 (2013) 125–131.
- [43] A. Moncayo-Lasso, J. Sanabria, C. Pulgarin, N. Benítez, N. Benítez, N. Benítez, Simultaneous *E. coli* inactivation and NOM degradation in river water via photo-Fenton process at natural pH in solar CPC reactor, A new way for enhancing solar disinfection of natural water, *Chemosphere*. 77 (2009) 296–300, <https://doi.org/10.1016/j.chemosphere.2009.07.007>.
- [44] E. Ortega-Gómez, M.M.B. Martín, B.E. García, J.A.S. Pérez, P.F. Ibáñez, Solar photo-Fenton for water disinfection: an investigation of the competitive role of model organic matter for oxidative species, *Appl. Catal. B Environ.* 148–149 (2014) 484–489, <https://doi.org/10.1016/j.apcatb.2013.09.051>.
- [45] M. Kohantorabi, S. Giannakis, M.R. Gholami, L. Feng, C. Pulgarin, A systematic investigation on the bactericidal transient species generated by photo-sensitization of natural organic matter (NOM) during solar and photo-Fenton disinfection of surface waters, *Appl. Catal. B Environ.* (2019) 983–995, <https://doi.org/10.1016/j.apcatb.2018.12.012>.
- [46] F.L. Rosario-Ortiz, S. Canonica, Probe compounds to assess the photochemical activity of dissolved organic matter, *Environ. Sci. Technol.* 50 (2016) 12532–12547, <https://doi.org/10.1021/acs.est.6b02776>.
- [47] E.A. Serna-Galvis, J.A. Troyon, S. Giannakis, R.A. Torres-Palma, C. Minero, D. Vione, C. Pulgarin, Photoinduced disinfection in sunlit natural waters: measurement of the second order inactivation rate constants between *E. Coli* and photogenerated transient species, *Water Res.* 147 (2018) 242–253, <https://doi.org/10.1016/j.watres.2018.10.011>.
- [48] S.L. Rosado-Lausell, H. Wang, L. Gutierrez, O.C. Romero-Maraccini, X.Z. Niu, K.Y. Gin, J.P. Croue, T.H. Nguyen, Roles of singlet oxygen and triplet excited state of dissolved organic matter formed by different organic matters in bacteriophage MS2 inactivation, *Water Res.* 47 (2013) 4869–4879, <https://doi.org/10.1016/j.watres.2013.05.018>.
- [49] Y. Lester, C.M. Sharpless, H. Mamane, K.G. Linden, Production of photo-oxidants by dissolved organic matter during UV water treatment, *Env. Sci Technol.* 47 (2013) 11726–11733, <https://doi.org/10.1021/es402879x>.
- [50] D. Vione, M. Minella, V. Maurino, C. Minero, Indirect photochemistry in sunlit surface waters: photoinduced production of reactive transient species, *Chem. – A Eur. J.* 20 (2014) 10590–10606, <https://doi.org/10.1002/chem.201400413>.
- [51] D. Vione, G. Falletti, V. Maurino, C. Minero, E. Pelizzetti, M. Malandrino, R. Ajassa, R.-I.I. Olariu, C. Arsene, Sources and sinks of hydroxyl radicals upon irradiation of natural water samples, *Environ. Sci. Technol.* 40 (2006) 3775, <https://doi.org/10.1021/es052206b>.
- [52] E. Ortega-Gómez, M.M.B.M.B. Martín, B.E. García, J.A.S.A.S. Pérez, P.F. Ibáñez, Wastewater disinfection by neutral pH photo-Fenton: the role of solar radiation intensity, *Appl. Catal. B Environ.* 181 (2016) 1–6, <https://doi.org/10.1016/j.apcatb.2015.06.059>.
- [53] C. Ruales-Lonfat, J.F. Barona, A. Sienkiewicz, J. Vélez, L.N. Benítez, C. Pulgarin, Bacterial inactivation with iron citrate complex: a new source of dissolved iron in solar photo-Fenton process at near-neutral and alkaline pH, *Appl. Catal. B Environ.* 180 (2016) 379–390, <https://doi.org/10.1016/j.apcatb.2015.06.030>.
- [54] D. Vione, M. Minella, C. Minero, V. Maurino, P. Picco, A. Marchetto, G. Tartari, Photodegradation of nitrite in lake waters: role of dissolved organic matter, *Environ. Chem.* 6 (2009) 407–415.
- [55] K. Finlay, R.J. Vogt, M.J. Bogard, B. Wissel, B.M. Tutolo, G.L. Simpson, P.R. Leavitt, Decrease in CO₂ efflux from northern hardwater lakes with increasing atmospheric warming, *Nature*. 519 (2015) 215.
- [56] R. Bhatia, D. Jain, Water quality assessment of lake water: a review, *Sustain. Water Resour. Manag.* 2 (2016) 161–173.
- [57] M. de Kwaadsteniet, P.H. Dobrowsky, A. van Deventer, W. Khan, T.E. Cloete, Domestic rainwater harvesting: microbial and chemical water quality and point-of-Use treatment systems, *Water Air Soil Pollut.* 224 (2013) 1629, <https://doi.org/10.1007/s11270-013-1629-7>.
- [58] S. Giannakis, E. Darakas, A. Escalas-Cañellas, C. Pulgarin, Solar disinfection modeling and post-irradiation response of *Escherichia coli* in wastewater, *Chem. Eng. J.* 281 (2015) 588–598, <https://doi.org/10.1016/j.cej.2015.06.077>.
- [59] A.H. Geeraerd, V.P. Valdramidis, J.F. Van Impe, GInaFit, a freeware tool to assess non-log-linear microbial survivor curves, *Int. J. Food Microbiol.* 102 (2005) 95–105.
- [60] E.A. Serna-Galvis, J.A. Troyon, S. Giannakis, R.A. Torres-Palma, L. Carena, D. Vione, C. Pulgarin, Kinetic modeling of lag times during photo-induced inactivation of *E. Coli* in sunlit surface waters: unraveling the pathways of exogenous action, *Water Res.* 163 (2019) 114894, <https://doi.org/10.1016/J.WATRES.2019.114894>.
- [61] M. Bodrato, D. Vione, APEX (Aqueous Photochemistry of environmentally occurring Xenobiotics): a free software tool to predict the kinetics of photochemical processes in surface waters, *Environ. Sci. Process. Impacts* 16 (2014) 732–740, <https://doi.org/10.1039/C3EM00541K>.
- [62] S.E. Braslavsky, Glossary of terms used in photochemistry, 3rd edition (IUPAC Recommendations 2006), *Pure Appl. Chem.* 79 (2007) 293–465, <https://doi.org/10.1351/pac200779030293>.
- [63] S.A. Loiselle, N. Azza, A. Cozar, L. Bracchini, A. Tognazzi, A. Dattilo, C. Rossi, Variability in factors causing light attenuation in Lake Victoria, *Freshw. Biol.* 53 (2008) 535–545, <https://doi.org/10.1111/j.1365-2427.2007.01918.x>.
- [64] W.E. Federation, A.P.H. Association, Standard Methods for the Examination of Water and Wastewater, Am. Public Health Assoc., Washington, DC, USA, 2005.
- [65] Z. Nan, Y. Huang, R.A.O. Zhu, Z. Xue-Liang, Fast detection of carbonate and bicarbonate in groundwater and lake water by coupled ion selective electrode, *Chinese J. Anal. Chem.* 44 (2016) 355–360.
- [66] D. Rubio, E. Nebot, J.F. Casanueva, C. Pulgarin, Comparative effect of simulated solar light, UV, UV/H₂O₂ and photo-Fenton treatment (UV-Vis/H₂O₂/Fe²⁺ + 3+) in the *Escherichia coli* inactivation in artificial seawater, *Water Res.* 47 (2013) 6367–6379, <https://doi.org/10.1016/j.watres.2013.08.006>.
- [67] P.A. Maraccini, J. Wenk, A.B. Boehm, Exogenous indirect photoinactivation of bacterial pathogens and indicators in water with natural and synthetic photosensitizers in simulated sunlight with reduced UVB, *J. Appl. Microbiol.* 121 (2016) 587–597, <https://doi.org/10.1111/jam.13183>.
- [68] R. Hardeland, B. Poeggeler, R. Niebergall, V. Zelosko, Oxidation of melatonin by carbonate radicals and chemiluminescence emitted during pyrrole ring cleavage, *J. Pineal Res.* 34 (2003) 17–25.
- [69] P. Sun, C. Tyree, C.-H. Huang, Inactivation of *Escherichia coli*, bacteriophage MS2, and *Bacillus* spores under UV/H₂O₂ and UV/peroxydisulfate advanced disinfection conditions, *Environ. Sci. Technol.* 50 (2016) 4448–4458.
- [70] D.B. Medinas, G. Cerchiaro, D.F. Trindade, O. Augusto, The carbonate radical and related oxidants derived from bicarbonate buffer, *IUBMB Life* 59 (2007) 255–262.
- [71] M. Gourmelon, J. Cillard, M. Pommepuy, Visible light damage to *Escherichia coli* in seawater: oxidative stress hypothesis, *J. Appl. Bacteriol.* 77 (1994) 105–112.
- [72] J. Kiwi, A. Lopez, V. Nadtochenko, Mechanism and kinetics of the OH-radical intervention during Fenton oxidation in the presence of a significant amount of radical scavenger (Cl⁻), *Environ. Sci. Technol.* 34 (2000) 2162–2168.
- [73] A. Zapata, I. Oller, E. Bizani, J.A. Sánchez-Pérez, M.I. Maldonado, S. Malato, Evaluation of operational parameters involved in solar photo-Fenton degradation of a commercial pesticide mixture, *Catal. Today* 144 (2009) 94–99.
- [74] R. Xiao, K. Liu, L. Bai, D. Minakata, Y. Seo, R.K. Göktas, D.D. Dionysiou, C.-J. Tang, Z. Wei, R. Spinney, Inactivation of pathogenic microorganisms by sulfate radical: present and future, *Chem. Eng. J.* (2019).
- [75] P. Neta, R.E. Huie, A.B. Ross, Rate constants for reactions of inorganic radicals in aqueous solution, *J. Phys. Chem. Ref. Data* 17 (1988) 1027–1284.
- [76] A. Bianco, M. Passananti, H. Perroux, G. Voyard, C. Mouchel-Vallon, N. Chaumerliac, G. Mailhot, L. Deguillaume, M. Brigante, A better understanding of hydroxyl radical photochemical sources in cloud waters collected at the puy de Dôme station—experimental versus modelled formation rates, *Atmos. Chem. Phys.* 15 (2015) 9191–9202.
- [77] C. Minero, S. Chiron, G. Falletti, V. Maurino, E. Pelizzetti, R. Ajassa, M.E. Carlotto, D. Vione, Photochemical processes involving nitrite in surface water samples, *Aquat. Sci.* 69 (2007) 71–85.
- [78] J. Ndounla, C. Pulgarin, Evaluation of the efficiency of the photo Fenton disinfection of natural drinking water source during the rainy season in the Sahelian region, *Sci. Total Environ.* 493 (2014) 229–238, <https://doi.org/10.1016/j.scitotenv.2014.05.139>.
- [79] J. Wang, M. Song, B. Chen, L. Wang, R. Zhu, Effects of pH and H₂O₂ on ammonia, nitrate, and nitrate transformations during UV254nm irradiation: implications to nitrogen removal and analysis, *Chemosphere*. 184 (2017) 1003–1011, <https://doi.org/10.1016/j.chemosphere.2017.06.078>.
- [80] C.C. Ryan, D.T. Tan, W.A. Arnold, Direct and indirect photolysis of sulfamethoxazole and trimethoprim in wastewater treatment plant effluent, *Water Res.* 45 (2011) 1280, <https://doi.org/10.1016/j.watres.2010.10.005>.
- [81] R.M. Dalrymple, A.K. Carfagno, C.M. Sharpless, Correlations between dissolved organic matter optical properties and quantum yields of singlet oxygen and hydrogen peroxide, *Environ. Sci. Technol.* 44 (2010) 5824–5829.
- [82] J. Porras, S. Giannakis, R.A. Torres-Palma, J.J. Fernandez, M. Bensimon,

- C. Pulgarin, Fe and Cu in humic acid extracts modify bacterial inactivation pathways during solar disinfection and photo-Fenton processes in water, *Appl. Catal. B Environ.* 235 (2018), <https://doi.org/10.1016/j.apcatb.2018.04.062>.
- [83] J.V. Goldstone, M.J. Pullin, S. Bertilsson, B.M. Voelker, Reactions of hydroxyl radical with humic substances: Bleaching, mineralization, and production of bioavailable carbon substrates, *Environ. Sci. Technol.* 36 (2002) 364–372.
- [84] D.M. McKnight, E.W. Boyer, P.K. Westerhoff, P.T. Doran, T. Kulbe, D.T. Andersen, Spectrofluorometric characterization of dissolved organic matter for indication of precursor organic material and aromaticity, *Limnol. Ocean.* 46 (2001) 38.
- [85] H.V. Lutze, S. Bircher, I. Rapp, N. Kerlin, R. Bakkour, M. Geisler, C. von Sonntag, T.C. Schmidt, Degradation of chlorotriazine pesticides by sulfate radicals and the influence of organic matter, *Environ. Sci. Technol.* 49 (2015) 1673–1680.
- [86] L. Zhou, M. Sleiman, C. Ferronato, J.-M. Chovelon, C. Richard, Reactivity of sulfate radicals with natural organic matters, *Environ. Chem. Lett.* 15 (2017) 733–737.
- [87] H.K. Trivedi, L.-K. Ju, Study of nitrate metabolism of *Escherichia coli* using fluorescence, *Biotechnol. Prog.* 10 (1994) 421–427.
- [88] A. Sekowska, H.-F. Kung, A. Danchin, Sulfur metabolism in *Escherichia coli* and related bacteria: facts and fiction, *J. Mol. Microbiol. Biotechnol.* 2 (2000) 145–177.
- [89] E.T. Bolton, D.B. Cowie, M.K. Sands, SULFUR METABOLISM IN *ESCHERICHIA COLI* III.: the metabolic fate of sulfate sulfur, *J. Bacteriol.* 63 (1952) 309.
- [90] J. Du, B. Förster, L. Rourke, S.M. Howitt, G.D. Price, Characterisation of cyanobacterial bicarbonate transporters in *E. Coli* shows that SbtA homologs are functional in this heterologous expression system, *PLoS One* 9 (2014) e115905.